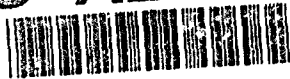
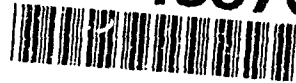


NAVY POSTGRADUATE SCHOOL
Monterey, California

AD-A280 395



94-18870



THESIS

Anode Sheath Contributions in Plasma Thrusters

by

John Forrest Riggs

March, 1994

Thesis Advisor:

Oscar Biblarz

Approved for public release; distribution is unlimited.

DTIC QUALITY INSPECTED 2

94 6 17 027

DTIC
SELECTED
JUN 20 1994
S B D

REPORT DOCUMENTATION PAGE

Form Approved OMB No. 0704

Public reporting burden for this collection of information is estimated to average 1 hour per response, including the time for reviewing instruction, searching existing data sources, gathering and maintaining the data needed, and completing and reviewing the collection of information. Send comments regarding this burden estimate or any other aspect of this collection of information, including suggestions for reducing this burden, to Washington Headquarters Services, Directorate for Information Operations and Reports, 1215 Jefferson Davis Highway, Suite 1204, Arlington, VA 22202-4302, and to the Office of Management and Budget, Paperwork Reduction Project (0704-0188) Washington DC 20503.

1. AGENCY USE ONLY (Leave blank)		2. REPORT DATE March 1994	3. REPORT TYPE AND DATES COVERED Engineer's and Master's Thesis	
4. TITLE AND SUBTITLE ANODE SHEATH CONTRIBUTIONS IN PLASMA THRUSTERS			5. FUNDING NUMBERS	
6. AUTHOR(S) Riggs, John Forrest				
7. PERFORMING ORGANIZATION NAME(S) AND ADDRESS(ES) Naval Postgraduate School Monterey CA 93943-5000			8. PERFORMING ORGANIZATION REPORT NUMBER	
9. SPONSORING/MONITORING AGENCY NAME(S) AND ADDRESS(ES)			10. SPONSORING/MONITORING AGENCY REPORT NUMBER	
11. SUPPLEMENTARY NOTES The views expressed in this thesis are those of the author and do not reflect the official policy or position of the Department of Defense or the U.S. Government.				
12a. DISTRIBUTION/AVAILABILITY STATEMENT Approved for public release; distribution is unlimited.			12b. DISTRIBUTION CODE A	
13. ABSTRACT (maximum 200 words) Contributions of the anode to Magnetoplasmadynamic (MPD) thruster performance are considered. High energy losses at this electrode, surface erosion, and sheath/ionization effects must be controlled in designs of practical interest. Current constriction or spotting at the anode, evolving into localized surface damage and considerable throat erosion, is shown to be related to the electron temperature's (T_e) rise above the gas temperature (T_0). An elementary one-dimensional description of a collisional sheath which highlights the role of T_e is presented. Computations to model the one-dimensional sheath are attempted using a set of five coupled first-order, nonlinear differential equations describing the electric field, as well as the species current and number densities. For a large temperature nonequilibrium (i.e., $T_e \gg T_0$), the one-dimensional approach fails to give reasonable answers and a multidimensional description is deemed necessary. Thus, anode spotting may be precipitated by the elevation of T_e among other factors. A review of transpiration cooling as a means of recouping some anode power is included. Active anode cooling via transpiration cooling would result in (1) quenching T_e , (2) adding "hot" propellant to exhaust, and (3) reducing the local electron Hall parameter. However, significant technical problems remain.				
			15. NUMBER OF PAGES 106	
			16. PRICE CODE	
17. SECURITY CLASSIFICATION OF REPORT Unclassified	18. SECURITY CLASSIFICATION OF THIS PAGE Unclassified	19. SECURITY CLASSIFICATION OF ABSTRACT Unclassified	20. LIMITATION OF ABSTRACT UL	

NSN 7540-01-280-5500

Standard Form 298 (Rev. 2-89)

Prescribed by ANSI Std. Z39-18

Approved for public release; distribution is unlimited.

Anode Sheath Contributions in Plasma Thrusters

by

John F. Riggs

Lieutenant Commander, United States Navy

B.A., University of Kansas, 1982

**Submitted in partial fulfillment
of the requirements for the degrees of**

AERONAUTICAL & ASTRONAUTICAL ENGINEER

and


MASTER OF SCIENCE IN ASTRONAUTICAL ENGINEERING

from the

NAVAL POSTGRADUATE SCHOOL

March 1994


Author:


John F. Riggs

Approved by:


Oscar Biblarz, Thesis Advisor


Fred Schwirzke, Second Reader


D.J. Collins, Chairman

Department of Aeronautical Engineering


Richard S. Elster, Dean of Instruction

ABSTRACT

Contributions of the anode to Magnetoplasmadynamic (MPD) thruster performance are considered. High energy losses at this electrode, surface erosion, and sheath/ionization effects must be controlled in designs of practical interest. Current constriction or spotting at the anode, evolving into localized surface damage and considerable throat erosion, is shown to be related to the electron temperature's (T_e) rise above the gas temperature (T_0). An elementary one-dimensional description of a collisional sheath which highlights the role of T_e is presented. Computations to model the one-dimensional sheath are attempted using a set of five coupled first-order, nonlinear differential equations describing the electric field, as well as the species current and number densities. For a large temperature nonequilibrium (i.e., $T_e \gg T_0$), the one-dimensional approach fails to give reasonable answers and a multidimensional description is deemed necessary. Thus, anode spotting may be precipitated by the elevation of T_e among other factors. A review of transpiration cooling as a means of recouping some anode power is included. Active anode cooling via transpiration cooling would result in (1) quenching T_e , (2) adding "hot" propellant to exhaust, and (3) reducing the local electron Hall parameter. However, significant technical problems remain.

Accession For	
NTIS GRA&I	<input checked="" type="checkbox"/>
DTIC TAB	<input type="checkbox"/>
Unannounced	<input type="checkbox"/>
Justification	
By _____	
Distribution/_____	
Availability Codes	
Dist	Avail and/or Special
A-1	

TABLE OF CONTENTS

I. INTRODUCTION	1
II. LITERATURE REVIEW	5
III. ANODE DESCRIPTION	7
A. THRUSTER GEOMETRY DESCRIPTION	7
B. ELEMENTARY SHEATH FORMULAE DESCRIPTION	11
1. Discussion	11
2. Simplified Formulation	14
3. Approximate Formulation	21
a. Effects of Temperature on Anode Constriction	22
(1) Case I: $T_e = T_i = T_o$ (Equilibrium)	23
(2) Case II: $T_e \gg T_i = T_o$ (Two-Temperature)	25
b. Similarity to Vacuum Arc Phenomena	27
C. COMPUTER CODE	29
D. COMPUTATIONAL RESULTS	30
E. ANODE FALL VOLTAGE	36
IV. TRANSPIRATION COOLING	38
V. CONCLUSIONS AND RECOMMENDATIONS	43

APPENDIX - APPLICABLE FORTRAN PROGRAMS	46
LIST OF REFERENCES	92
INITIAL DISTRIBUTION LIST	96

LIST OF TABLES

I. NOMENCLATURE	15
-----------------------	----

LIST OF FIGURES

1. Magnetoplasmadynamic (MPD) Thruster	8
2. Space Plasma Thruster	10
3. Electric Field Between Two Electrodes	11
4. Electric Field and First Two Space Derivatives	19
5. Electric Field and Species Approximation	24
6. Two-dimensional Model of Current Paths	26
7. Anode Discharge Modes	28
8. Ionization Coefficient ν as a Function of E/N	30
9. Species Number Density Plots for Individual Computer Run	32
10. Electric Field as a Function of γ	34
11. Species Number Density as a Function of γ	35

ACKNOWLEDGMENT

I dedicate this work to my dear wife Lin, for her support and understanding during my absence as a geographical bachelor of almost three years.

My sincere thanks to my parents for encouraging me to pursue my ambitions from childhood on, and to Oscar Biblarz, Ph.D., for patiently helping me to understand plasma physics.

I. INTRODUCTION

Several types of space flight propulsion systems have been developed over the years. These include chemical, nuclear, electric and solar propulsion. The majority of space thrusters to date have been chemical rockets. Although the Chinese used rockets over 800 years ago, true development of rocket propulsion took place during this century [Ref. 1]. Chemical thrusters give high thrust-to-weight ratios, larger than unity, and have been fully developed in the form of space launch vehicles and attitude control thrusters. In contrast, other propulsion systems have been developed only to the proof-of-concept stage, and essentially remain at this stage of development. Nuclear propulsion was studied with the NERVA (Nuclear Engine for Rocket Vehicle Application) thruster in the 1960's, and abandoned [Ref. 2:pp. 517-519]. Electric propulsion flights during the 1960's included the U.S. SERT-1 (Space Electric Rocket Test) in 1964 and the U.S.S.R. Yantari-1 rocket in 1966. Solar-electric propulsion was demonstrated via the SERT-2 rocket in 1970, powering the electric thruster from power generated by solar cells. Further electric propulsion research flights in the 1980's included the U.S. Navy's NOVA-1 satellite in 1981, and Japan's MS-T4 satellite, launched from the Space Shuttle. Beyond this, nonchemical thrusters have only been used in auxiliary roles, such as station-keeping and attitude

control on geosynchronous satellites. NASA's Project PATHFINDER in the mid-1980's proposed the use of a megawatt-level electric plasma thruster for a manned Mars mission. However, development of this project was never funded.

In comparing the different propulsion schemes, a primary performance indicator is specific impulse, defined as the ratio of thrust to the rate of propellant usage, or alternately, propellant effective exhaust velocity (u_e), divided by the sea-level gravitational constant, (g_0).

$$I_{sp} = \frac{\dot{m} u_e}{\dot{m} g_0} = \frac{u_e}{g_0} \quad \text{sec} \quad (1)$$

Chemical rockets are inherently limited in performance by the total energy available in the fuel/oxidizer combustion process, so that the total enthalpy available for conversion into exhaust kinetic energy is limited. Exhaust velocity is also limited by material heating limitations of the combustion chamber and nozzle throat, and "frozen flow Losses" (unrecoverable energy deposition in internal modes of the gas) [Ref. 3:pp. 4-5]. Peak specific impulse for liquid chemical propellants is presently on the order of 450 seconds. This capability is completely sufficient for the tasks of launch to low earth orbit (LEO), attitude control, station keeping, and such missions. However, for missions such as manned interplanetary exploration, chemical propulsion can be shown to be clearly inadequate. A comparative analysis of a Mars

mission using chemical and electric propulsion systems shows the large difference in mass payload ratio (final mass/initial launch mass) for the two systems. A chemical system using a high impulse Hohman ellipse trajectory delivers a maximum of approximately 10% to 18% of the launch mass to the Martian surface [Ref. 4:p. 115]. In comparison, an electric system using a low impulse spiral trajectory could deliver from 20% to 60% of the launch mass, depending on the desired transit time. Each mission assumes transit from low Earth orbit to Mars orbit. An electric propulsion system would still need a high thrust propulsion system to reach the Martian surface [Ref. 5:pp. 344-346]. The large difference in payload ratio is due to the much larger exhaust velocity and more efficient use of fuel by electric propulsion. Thus, some form of electric or hybrid electric thruster would seem to be in order for such interplanetary missions. However, due to the low thrust-to-weight ratio of electric thrusters, they must be launched into orbit by other means. Their usefulness is restricted to space thrusters, not to launch systems.

With specific impulses of as high as 10,000 seconds, electric propulsion offers the performance envelope needed for manned interplanetary missions. Electric propulsion is divided into three types of thrusters: electrostatic, electrothermal, and electromagnetic. The type relevant to this work is the magnetoplasmadynamic (MPD) thruster, an electromagnetic propulsion system that utilizes the Lorentz force created by an electric current together with its induced magnetic field to propel a gas that has been heated to the plasma state. According to electromagnetic theory, a conductor carrying a current produces an induced magnetic force perpendicular to

the current. The applied electric field and its induced magnetic field interact to produce the Lorentz force ($\vec{F} = \vec{j} \times \vec{B}$) perpendicular to both fields on the conductors. This briefly summarizes the concept behind the "self-field" MPD accelerator [Ref. 2:pp. 485-486]. MPD performance is enhanced by adding magnetic coils to the thruster, thus strengthening the magnetic field and, as a consequence, the Lorentz force and thrust. This thruster is appropriately called an "applied-field" MPD thruster. MPD thrusters have shown specific impulses of up to 7,000 seconds and efficiencies as high as 70% [Ref. 6:pp. 2-3]. Performance of MPD thrusters is limited by several factors, including electrode erosion, current spotting, frozen flow losses, and electrode power deposition. Specifically, anode power deposition is the single largest power loss mechanism in MPD thrusters operating at submegawatt power levels [Ref. 7]. In the following work, we review and analytically model the MPD anode, including the sheath and anode potential drop.

II. LITERATURE REVIEW

Anode losses significantly limit magnetoplasmadynamic (MPD) thruster performance. Much effort has been placed on characterizing these losses and on the nature of power deposition in the anode [Refs. 8-14]. As much as 80% of thruster total power may end up being deposited in the anode at sub-megawatt power levels [Refs. 8,15]. This power deposition together with current constriction at the anode surface present serious problems to thruster cooling and performance, as well as to anode lifetime. Before any practical design can be achieved, a more thorough understanding of the phenomena at the anode, particularly the anode sheath, must be gained. Studies have shown that the anode power fraction depends on thruster power, current, mass flow rate, and the parameter J^2/\dot{m} [Refs. 8,12,13,16]. It has also been shown that the anode fall voltage is inversely proportional to anode current density [Refs. 13,16]. It is believed that a better understanding of the role of an elevated electron temperature, of current flow dimensionality, and of current unsteadiness are prerequisites for the evolution of any practical MPD thruster design.

Computer codes that accurately describe observed data from steady-state MPD thrusters have been developed [Refs. 17-19]. However, these codes do not adequately describe observed data from quasi-steady thruster experiments. It has been suggested that the lack of proper electrode modelling (i.e., sheaths and fall potentials) in these

codes may explain this discrepancy [Ref. 6]. Limited analytical work has been done in modelling the sheath and ambipolar regions at the anode, influenced perhaps by the difficult set of coupled, nonlinear partial differential equations involved. Hugel [Ref. 12] and Subramaniam [Ref. 20] address the influence of the sheath region, but do not model the electric field, temperature, or sheath fall voltage.

Given the minuscule extent of the sheath versus thruster anode curvature, the problem at first appears one-dimensional in nature. A one-dimensional, collisional, equilibrium solution can satisfactorily reproduce the observed electric field and charge density distributions for the entire sheath and ambipolar regions for a sheath where the electron temperature equals that of the heavy species [Ref. 21]. However, this model cannot describe any decrease in current density away from the surface, or current constriction, at the anode surface which might be necessary in nonequilibrium. A two-dimensional model, developed by Biblarz and Dolson [Ref. 14], represents these phenomena and predicts the voltage drop in the region. It is shown that the sheath must account for a majority of the anode voltage drop, and that the sheath extent must be greater than the Debye length [Refs. 14,21]. Thus, a combination of one- and two-dimensional approaches appears to better describe sheath behavior. Incorporation of modelling of this sort may improve the ability of the computer codes cited above to properly describe quasi-steady thrusters.

Next, a description of the anode region is presented in order to delineate some of the possible effects of temperature.

III. ANODE DESCRIPTION

A. THRUSTER GEOMETRY DESCRIPTION

The majority of plasma thrusters to date have consisted of a central cathode rod surrounded by an annular shell anode, as shown in Figure 1 [Ref. 23]. The thruster illustrated is sufficient to produce needed thrust at current levels above one kiloamp. Below this level, an external magnetic field produced by an annular magnet is needed to ensure sufficient Lorentz force on the plasma propellant to meet thrust requirements. [Ref. 8]. As illustrated in Figure 1, the $\vec{j} \times \vec{B}$ body force simplifies into an axial ($j_z B_\theta$) body force, which provides direct electromagnetic thrust ("blowing"), and a radial ($-j_r B_\theta$) body force, which provides electromagnetic compression of the plasma and a subsequent pressure force along the cathode surface ("pumping"). [Ref. 6]

A notable exception to this geometry is the Stationary Plasma Thruster (SPT), a design from the former Soviet Union. The SPT is an example of a plasma propulsion system known as a Hall Current Plasma accelerator. An electric field is applied axially to a stream of flowing plasma, in addition to a magnetic field with a strong radial component, which is applied by an external electromagnet. When the axial electric field is applied and a current flows through the plasma, an azimuthal component of current is induced, i.e., the "Hall" current.

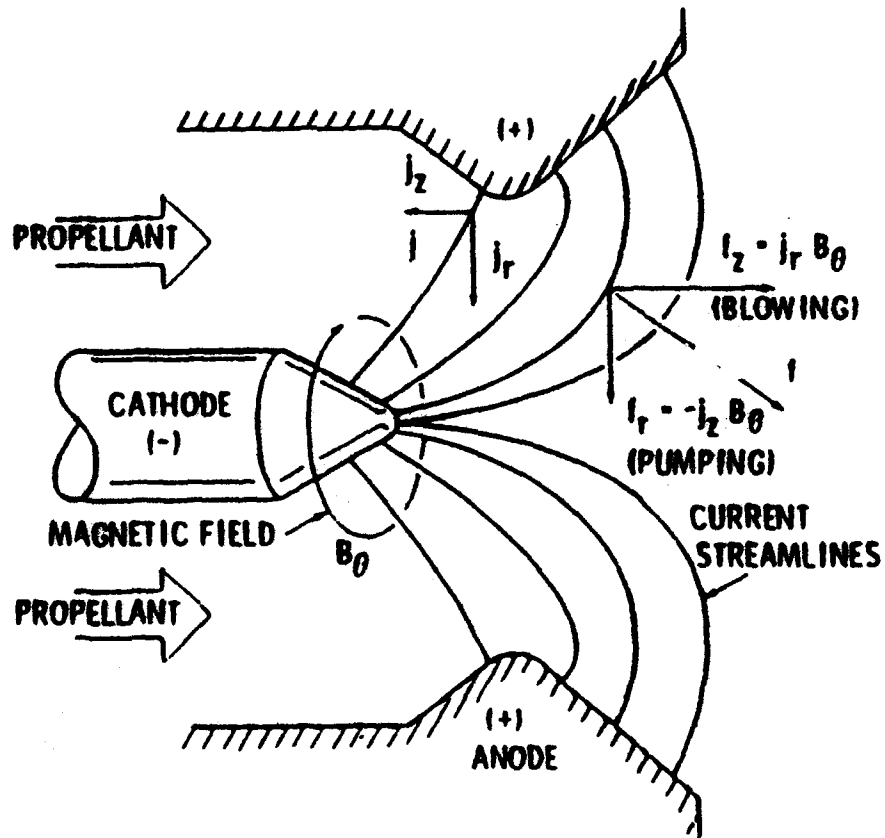


Figure 1 - Magnetoplasmadynamic (MPD) Thruster, with Axial and Radial Forces on Plasma Indicated. [Ref. 23]

Thrust is produced by electrostatically accelerating the ions in the plasma, as well as through the induced Lorentz force mentioned above. A strong radial magnetic field is applied to the plasma, whose properties are controlled to make the electron Larmor radius¹ small compared to the mean free path², while the ion Larmor radius is comparatively large. As a consequence, electron mobility in the axial direction is greatly reduced. Thus, the electric field energy is given mainly to the ions, producing axial ion acceleration. Collisions with neutral particles serve to accelerate the entire neutral plasma. [Ref. 24]

A pair of the final prototype design developed, the SPT-100, have been acquired by NASA recently from Fakel Enterprise in Kaliningrad, Russia, and are undergoing performance evaluation at the Jet Propulsion Laboratory. Designed at the Kurchatov Institute of Atomic Energy (IAE) in Moscow, USSR in the 1960's, smaller versions of the SPT-100 (SPT-50 and SPT-70) were flown beginning in 1972³. A specific impulse of 1,600 seconds and 50% efficiency, as well as space flights of fifty similar thrusters is claimed. The specific operational characteristics of the thruster are not well understood presently. Bohm diffusion of electrons and a phenomenon called "near-wall conductivity" have been proposed to explain the thruster's operation. This thruster is shown in Figure 2. [Ref. 25]

¹ Larmor radius is the radius of the helix traversed by a charged particle moving in a magnetic field.

² Mean free path is the distance traveled by a particle before making a collision.

³The suffix (i.e., "-70") indicates the characteristic diameter of the thruster in millimeters.

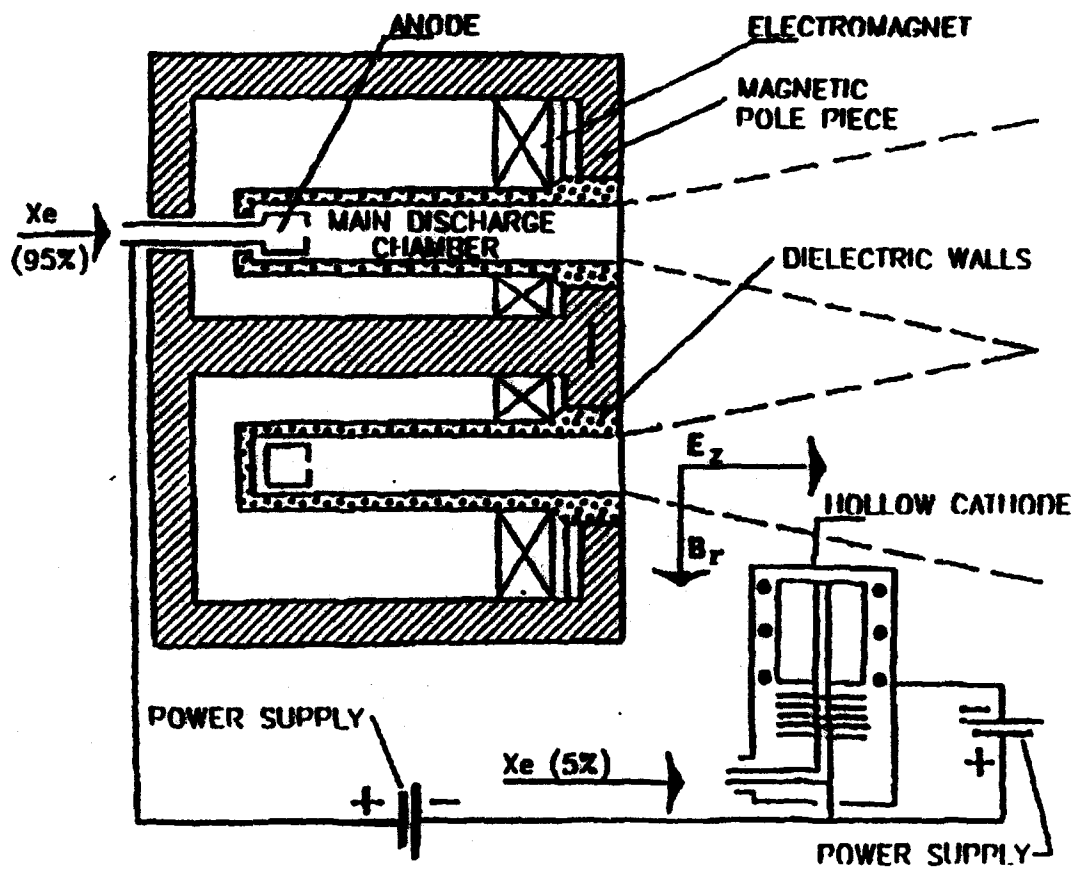


Figure 2 - Stationary Plasma Thruster [Ref. 25]

B. ELEMENTARY SHEATH FORMULAE DESCRIPTION

1. Discussion

Voltage losses and anode power deposition account for most of the inefficiency of plasma thrusters. In order to understand these losses, the anode region must be understood and related phenomena explained and modelled. As shown in Figure 3, a substantial drop in voltage occurs in a short distance from the anode surface.

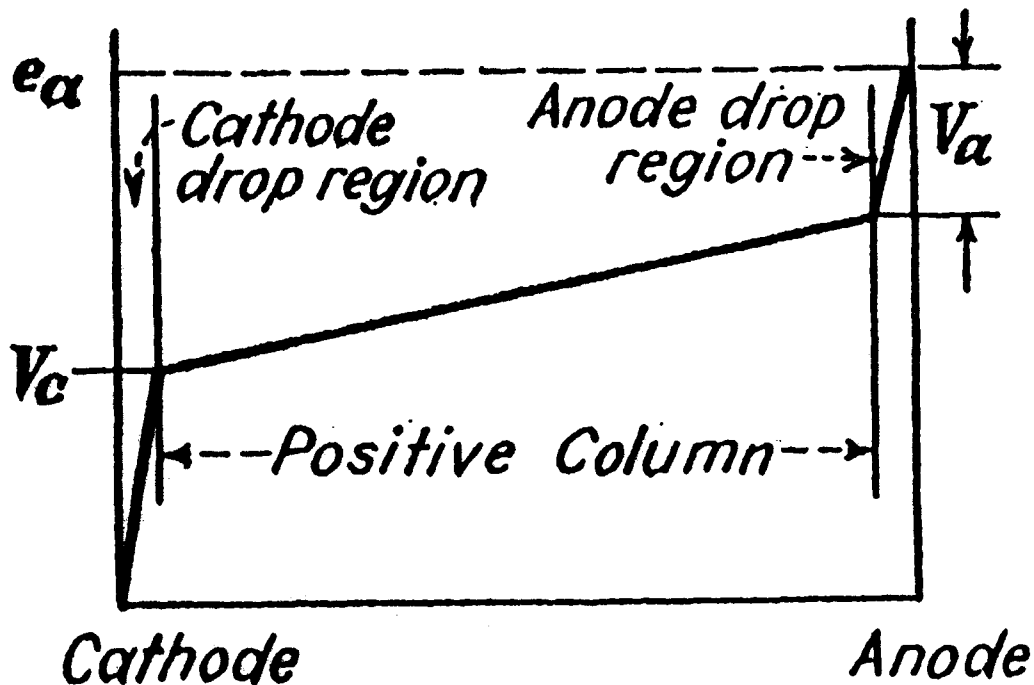


Figure 3 - Electric Field Between Two Electrodes, Including "Positive Column". [Ref. 27]

The anode fall region may be divided into two parts, the sheath and ambipolar regions. The plasma attempts to adjust itself near electrodes so as to shield the main body of the plasma from the electric field [Ref. 26]. The sheath is the region closest

to the anode surface within which the ion and electron number densities are unequal, with the electrons dominating the region. A high electron space charge exists at the anode surface. This is caused by the anode collecting incoming electrons in completing the arc current with the cathode. Positive ions are produced within the sheath by electron impact of neutral gas molecules, and the ions are repelled toward the cathode. At the cathode end of the anode drop region, the density of positive ions is high enough to almost neutralize the electron space charge, thus forming the positive column or core plasma. The essential positive ion current is created in this way near the anode. A more complete description of this process may be found in Cobine [Ref. 27] and von Engel [Ref. 28]. A fundamental characteristic of plasma behavior is its tendency toward electrical neutrality. Whenever local charge concentrations arise or external potentials are introduced into a system, these are shielded out in a distance known as the "Debye length". This distance must be much smaller than the system dimension for the ionized gas to be considered a plasma [Ref. 29]. Equation (2) gives the Debye length [Ref. 26].

$$\lambda_d = \sqrt{\frac{\epsilon_0 kT}{n_e e^2}} = 69.0 \sqrt{\frac{T}{n_e}} \quad (\text{m}) \quad (2)$$

*The Debye length effectively describes the radius of a shell around a charged particle outside of which the potential of the particle is not seen.

Another distance of interest is the electron mean free path, or distance traveled by a particle before making a collision. Equation (3) is from a derivation of Lin, Resler, and Kantrowitz [Refs. 30,31] giving the mean free path, with λ_s being the approximate sheath length.

$$\lambda = 0.12 \left(\frac{1}{n_e (e^2/3kT)^2 \ln(\lambda_s e^2/3kT)} \right) \quad (3)$$

Since the sheath extends at most a few mean-free lengths from the anode surface, curvature of the anode does not affect the governing equations in high pressure discharges. Thus, the region may be described in one dimension, the distance "y" from the anode surface. While the Debye length is sometimes assumed as the sheath extent, Reference 22 showed that the sheath thickness is a function of the anode fall voltage and the electron temperature. Equation (4) gives the appropriate form.

$$\lambda_s = \sqrt{\frac{\epsilon_0 \Phi_a}{en_e}} = \lambda_D \sqrt{\frac{e\Phi_a}{kT_e}} \quad (4)$$

An example case with a fall voltage of 100 volts gives a sheath extent of $\lambda_s = 2.352 \times 10^{-5} \text{ m}$. This compares to a computed Debye length of $\lambda_D = 1.690 \times 10^{-6} \text{ m}$. Therefore, the sheath can be an order of magnitude larger than the Debye length.

Nasser [Ref. 32] discusses an elementary theoretical approach to the glow discharge problem. He suggests a set of four one-dimensional ordinary differential equations, including the electron and ion current and number density equations, in addition to Poisson's equation. Most solution attempts have failed, with the boundary conditions being identified as the culprit. A similar attempt for the plasma thruster is discussed below.

2. Simplified Formulation

The steady probe equations are first written [Ref. 21] in their simplest form. The anode is assumed to operate as a heavily biased probe, which is true for low enough currents when the anode is not a source of ions. Whenever the temperature can be considered fixed, the energy equations are implicitly satisfied and, since ion inertia is neglected, the resulting set consists only of two species continuity equations and Poisson's equation. These equations are written in terms of y , which is the coordinate outward from the planar positive surface. Constants and variables are listed in Table 1.

TABLE 1 - NOMENCLATURE

a... characteristic length of plasma	n_e... species number density at core plasma
$D_{i,e}$... species diffusion coefficient	N... total number density
e... elementary charge constant	T... temperature
E... electric field	T_0... neutral species temperature
E_0... electric field at anode surface	α... two-body recombination coefficient
E_c... electric field at core plasma	ϵ_0... permittivity constant
$j_{i,e}$... species current density	ν... ionization coefficient
J... total current	$\mu_{i,e}$... species mobility coefficient
k... Boltzmann's constant	Φ_a... anode fall potential
K... current parameter	λ... mean-free distance
$n_{i,e}$... species number density	λ_d... Debye length
\dot{n}_e... time rate-of-change of n_e	λ_s... Sheath thickness

Note: Species subscripts denote ions (i) and electrons (e).

$$j_i = e\mu_i n_i E - (eD_i) \frac{dn_i}{dy} \quad (5)$$

$$j_e = e\mu_e n_e E + (eD_e) \frac{dn_e}{dy} \quad (6)$$

$$\frac{dE}{dy} = \frac{e}{\epsilon_0} (n_i - n_e) \quad (7)$$

$$J = j_i + j_e \quad (8)$$

$$\mu_{i,e} = \frac{eD_{i,e}}{kT_{i,e}} \quad (9)$$

Here, the j 's are species contributions to the total current density. The existence of negative charges as free electrons is pivotal in the formulation. Next, the Einstein relation, equation (9), is introduced to write the mobilities in terms of the diffusion coefficients. We assume that the diffusion coefficients remain constant in the problem.

Equations (5) and (6) are next solved for $dn_{i,e}/dy$. The species current density equations are found from the net reaction rate of the plasma. Equations (10) and (11) combine to produce space derivatives for species current density.

$$\dot{n}_s = v_i n_s - \alpha n_i n_s \quad (10)$$

$$\frac{dj_s}{dy} = \frac{-dj_s}{dy} = e \dot{n}_s \quad (11)$$

Combining equations (5)-(11) produces a set of five coupled, non-linear differential equations describing the sheath. These are nondimensionalized to adjust all variables to the first order, and are rewritten below as equations (12)-(16), with nondimensionalized variables denoted by "x". Nondimensionalization can be accomplished as follows: The species number densities n_i, n_s , are divided by their values at infinity to produce output from the anode surface to unity at the ambipolar boundary. The current densities j_i, j_s are divided by the total current, allowing the output to show the "mirror behavior" of the two currents. The electric field is divided by the initial anode value to give output starting from unity at the surface and decreasing to the final core field value. The variable "y" is divided by the characteristic length³ of the plasma, "a", producing \bar{y} . These corrections allow all output to vary in the range from zero to one, as a function of distance from the anode.

³The characteristic length is defined so as to cancel the multiplying factor in the electric field equation, (14), ($a = 1.107 \times 10^6$). This allows a physical interpretation of the ion/electron number densities, as well as the decay rate of the electric field.

$$\frac{d\tilde{n}_i}{dy} = \left(\frac{aeE_0}{kT_0} \right) \tilde{n}_i \tilde{E} - \left(\frac{aeE_0}{kT_0} \right) \tilde{j}_i \quad (12)$$

$$\frac{d\tilde{n}_e}{dy} = - \left(\frac{aeE_0}{kT_0} \right) \tilde{n}_e \tilde{E} + \left(\frac{aeE_0}{kT_0} \right) \tilde{j}_e \quad (13)$$

$$\frac{d\tilde{E}}{dy} = \left(\frac{aen_0}{E_0 \epsilon_0} \right) (\tilde{n}_i - \tilde{n}_e) \quad (14)$$

$$\frac{d\tilde{j}_e}{dy} = - \left(\frac{akT_0 v_i}{eE_0 D_i} \right) \tilde{n}_e (\tilde{v}_i - \alpha \tilde{n}_i) \quad (15)$$

$$\frac{d\tilde{j}_i}{dy} = \left(\frac{akT_0 v_i}{eE_0 D_i} \right) \tilde{n}_i (\tilde{v}_i - \alpha \tilde{n}_i) \quad (16)$$

Attempts to solve this equation set using the computer code discussed below shows the set to be extremely sensitive to initial conditions. The computer code solver uses a "marching" scheme from the anode to the undisturbed plasma. The initial conditions are chosen to produce the electric field potential drop observed in actual thrusters. First and second space derivatives of the electric field are used as diagnostic checks to ensure reasonable output values and indicate instability of the integration process. Figure 4 shows the required resulting curves for the electric field and its first and second derivatives.

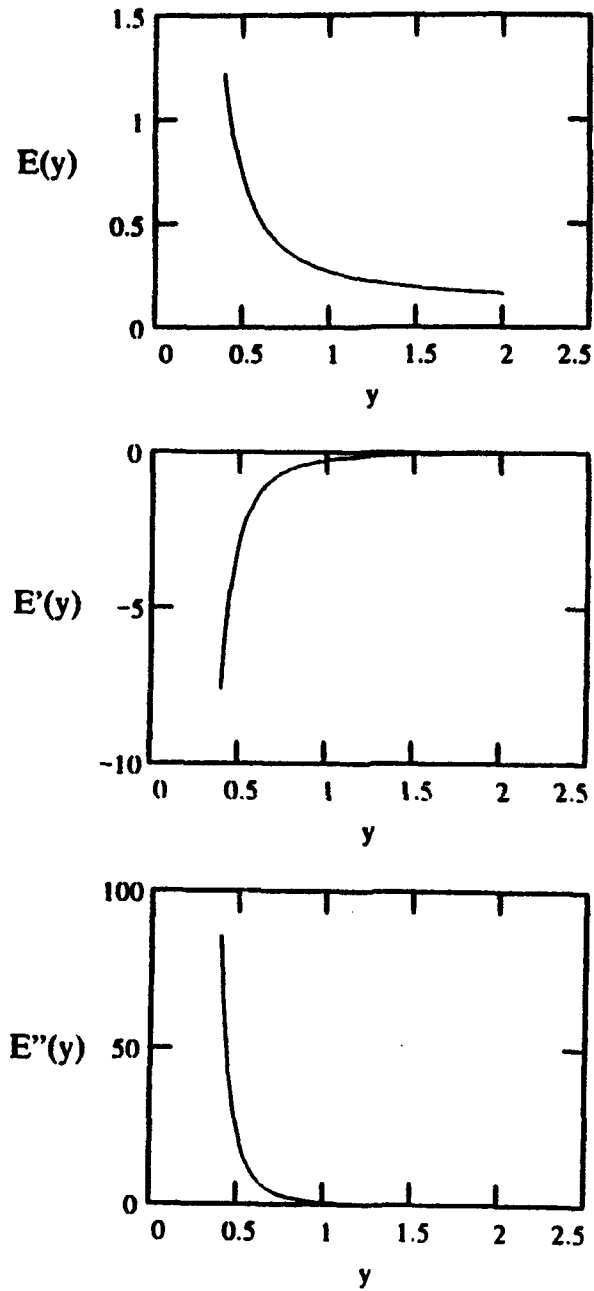


Figure 4 - Electric Field and First Two Space Derivatives Used as Diagnostic Checks for Integrator Output. (Plotted for a Generic Exponential Function).

Ecker characterizes the plasma at the anode as a double sheath, with the inner section called the "inertia sheath", and an outer section called the "energy loss section". The inner section shows a potential rise of the order of one volt, with the outer section showing the exponential potential drop shown in Figure 4. While this double sheath may in fact describe the actual sheath region, the formulation above only models the potential drop portion of the sheath, and does not attempt to produce the potential rise of the inner sheath. In addition, Ecker's current constrictions are of a "macroscopic" nature, whereas those of Reference 14 and this work are "microscopic" [Ref. 33].

Data for a 6,000°K Nitrogen plasma were used to test the equation set [Ref. 21]. Producing a proper solution required adjusting the initial conditions to force the curve shapes discussed above. Using Equations (2), (3), and (4), the mean free path, Debye length, and approximate sheath extent are calculated as $\lambda = 9.352 \times 10^{-3}$ m, $\lambda_D = 1.690 \times 10^{-6}$ m, and $\lambda_s = 2.352 \times 10^{-5}$ m (this assumes a drop voltage of 100 volts).

3. Approximate Formulation

Reference 21 explores the above equation set by taking advantage of the symmetry among the equations, and introducing two parameters, K^+ and K^- , shown below.

$$K^+ \equiv \frac{j_i}{eD_i} + \frac{j_e}{eD_e} \quad (17)$$

$$-K^- \equiv \frac{j_i}{eD_i} - \frac{j_e}{eD_e} \quad (18)$$

It can be shown that the resulting equations can be manipulated to yield a single, ordinary differential equation for the K 's in terms of the electric field. The resulting equation can be scrutinized for two distinct temperature regimes. Note that while the total current density, J , is constant in a steady, one-dimensional case, the K 's can vary and will in turn also depend on the degree of reactivity of the plasma (n_0), i.e.,

$$\frac{dj_i}{dy} = \frac{-dj_e}{dy} = en_0 \quad (19)$$

Because ion diffusion is much slower than electron diffusion, it can be shown that the K 's are related by

$$K^+ \approx -K^- + \frac{2J}{eD_e} \quad (20)$$

As will be evident, at the electrode surface the K 's are equal to each other and at the undisturbed plasma, $K^- = 0$. The total current density may be evaluated from

$$J = en_e v_{e0} \quad (21)$$

where v_{e0} is the electron drift velocity beyond the ambipolar region which is strictly a function of E_0/N , (i.e., of the ratio of undisturbed electric field to the total number density).

a. Effects of Temperature on Anode Constriction

It is useful to investigate the overall effects of temperature. Since temperature will be considered constant, it comes in as a parameter in this formulation whereas charge density and electric field remain as variables. Intuitive arguments will be introduced which suggest that the electron and ion/neutral temperatures play a rather singular role in determining the intrinsic dimensionality of the problem, (i.e., there are cases when the geometry of the current lines is not necessarily impressed by the electrode geometry). Since the problem is described by moderate pressure, largely collisional sheaths, the ion and neutral temperatures are anticipated to remain reasonably equal. Depending on the gas, the electron temperature, on the other hand, can be elevated from the gas temperature at the anode where actual magnitudes depend on the local value of E/N . In order to get a perspective on the effects of temperature, we shall consider two extremes, namely, the case where the electron and ion temperature are the same (the equilibrium case) and the case where the electron temperature is substantially elevated from that of the ions/neutrals (the two-temperature case).

(1) *Case I: $T_e = T_i = T_0$ (Equilibrium)*

The charge densities can be eliminated by combining equations (5)-(9), (17) and (18). The resulting equation can be shown to be

$$\frac{kT_0}{e} \left(\frac{K'}{E} \right)' + K' = \frac{2J}{eD_e} - \left(\frac{kT_0 \epsilon_0}{e^2} \right) \frac{1}{E^2} \left[EE'' - (E')^2 - \frac{1}{4} \left(\frac{e}{kT_0} \right)^2 E^4 \right] \quad (22)$$

If the electric field decreases monotonically from the wall to the undisturbed plasma (i.e., from $E_0 \rightarrow E_\infty$), then as $y \rightarrow \infty$, $E \rightarrow E_\infty$, $E' \rightarrow 0$, $E'' \rightarrow 0$.

So that in equation (22) above the "outer solution" becomes:

$$K' = \frac{2J}{eD_e} \quad (23)$$

Now this represents an acceptable solution from a physical point of view. Moreover, as $y \rightarrow \infty$,

$$\dot{n}_e \approx D_e (K')' \approx 0 \quad (24)$$

which is also acceptable for an equilibrium situation at the undisturbed plasma. Results [Ref. 21] are shown in Figure 5 for the case of nitrogen at 6000°K using an approximate electric field distribution.

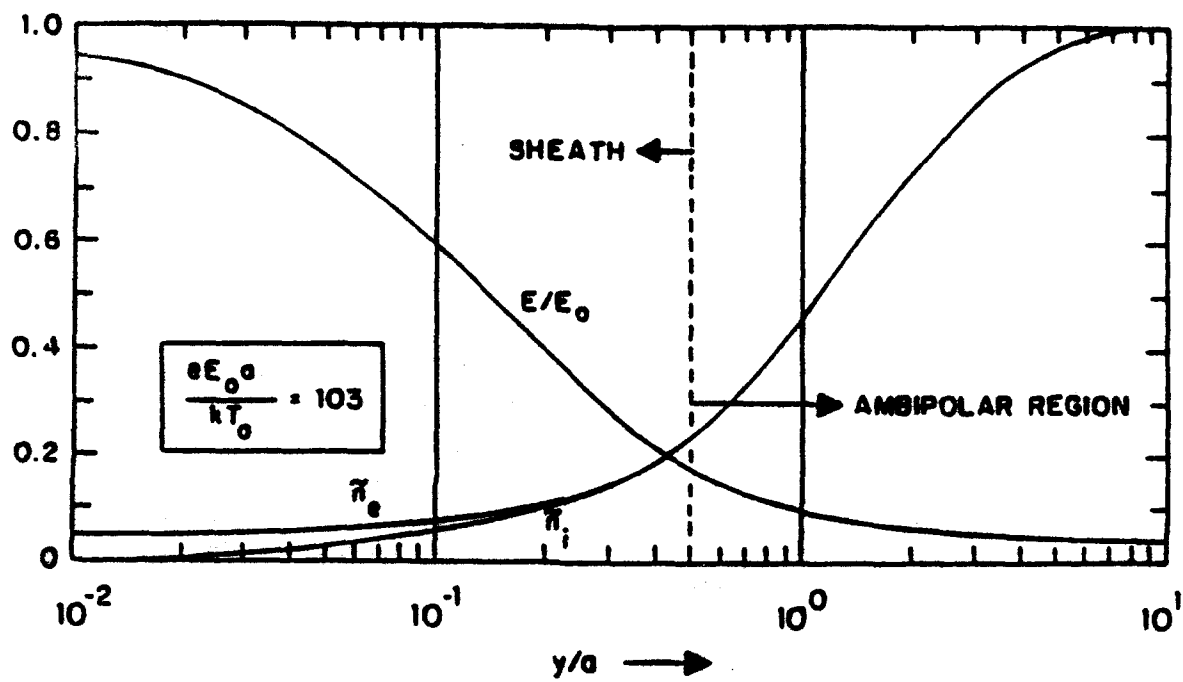


Figure 5 - Electric Field and Species as a Function of y , Distance From Anode. An Approximation Using a Shaped Electric Field and Isothermal Plasma [Ref. 21].

(2) *Case II: $T_e \gg T_i = T_0$ (Two-Temperature)*

In this case the same procedure as before yields the following equation where terms divided by T_i have been dropped when compared to their counterparts divided by T_0 .

$$(K^*)' - \frac{K^*}{E} E' = \frac{2EJ}{kT_0 D_0} + \frac{2\epsilon_0}{kT_0} EE'' + \frac{\epsilon_0}{eE} E''E' - \frac{\epsilon_0}{e} E''' \quad (25)$$

Assuming the same monotonic decrease as before for the electric field from the wall to the plasma proper, as $y \rightarrow \infty$, $E \rightarrow E_\infty$, $E' \rightarrow 0$, $E'' \rightarrow 0$.

Then the outer solution becomes

$$\frac{dK^*}{dy} = \frac{2eEJ}{kT_0 e D_0} \quad \text{with } \dot{n}_{\infty} > 0 \quad (26)$$

Or, $K^* \rightarrow (\text{constant}) y + \text{constant}$, and \dot{n}_{∞} keeps increasing with y .

This is not the proper outer solution for the one-dimensional, equilibrium plasma that we seek because the net ionization rate continues to increase well inside the plasma proper where conditions should saturate, yielding a constant electric field. Therefore, as formulated, Case II is not amenable to a one-dimensional solution. References 14 and 21 show how this case can be analyzed under a multidimensional approach. These references also discuss a method for describing the electron temperature as a function of E/N , then how to couple a simplified energy relation which satisfactorily describes a two-temperature plasma. The necessary ingredient to make equation (26) approach zero beyond the decrease of E to E_∞ is to allow J

to fan out as indicated in Figure 6. Thus, in equation (26), the product "EJ" can bring down the charge production rate to arbitrarily low values. Alternatively, it is possible to explore techniques of bringing the electron temperature down to be in closer equilibrium with the ions and neutrals. Transpiration cooling is one such means.

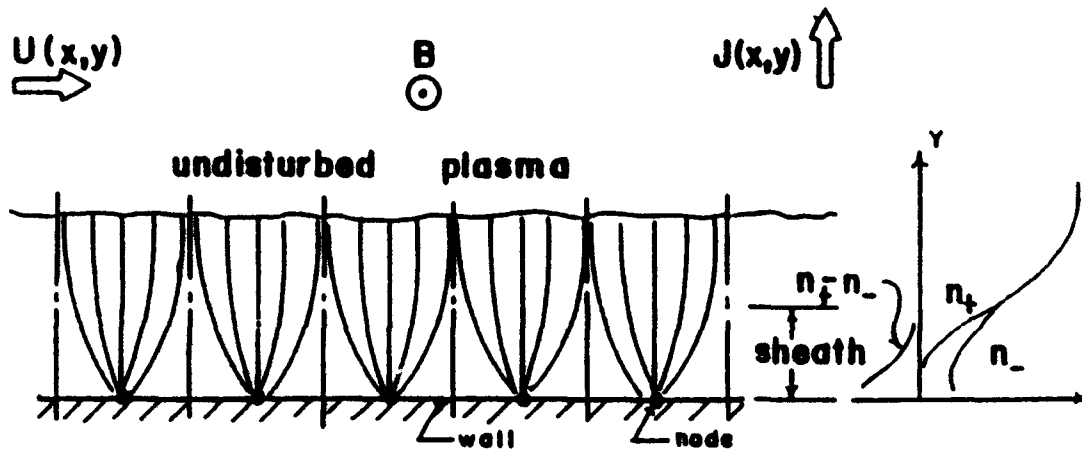


Figure 6 - Two-Dimensional Model of Current Paths Showing Periodic Structure. Thermal Instabilities and Inhomogeneities Would Favor One Site Over Others and a Single Macroscopic Constriction May Then Be Produced. [Refs. 14, 34]

b. *Similarity to Vacuum Arc Phenomena*

Instability phenomena observed in vacuum arcs [Ref. 35] are very similar to those observed in self-field thrusters [Ref. 12]. After the establishment of the current, the anode region operates in a vapor that issues from the electrodes. In vacuum arcs, Miller characterizes the anode region as operating in one of five distinct modes, ranging from a passive, low current mode to a high current, fully developed spot mode [Ref. 36]. Given the similarities mentioned above, vacuum arc anode research should be helpful in the understanding of MPD thruster transition to the anode spot mode. Existence diagrams after Miller [Ref. 36] are shown in Figure 7, which divide operating modes into regions as a function of anode current versus electrode geometry. Figure 7 shows the transition from glow to spot mode.

Anode spot formation at high currents is clearly a factor in limiting anode lifetime. Various phenomena have been related to anode spotting. Hugel [Ref. 12] relates the transition to spotting mode to an increase in J^2/\bar{m} above a critical level. A separate factor connected with the spot mode is surface temperature of the anode. Rich, et.al., [Ref. 37] show that anode spotting is preceded by a luminous "footpoint" and followed by local melting prior to spot formation. Separately, Schuocker [Ref. 38] finds a connection between spotting initiation and the factors of anode evaporation and magnetic constriction in vacuum arcs with high currents. Experimental investigations must be performed to see if the above-mentioned vacuum arc criteria apply to self-field thrusters.

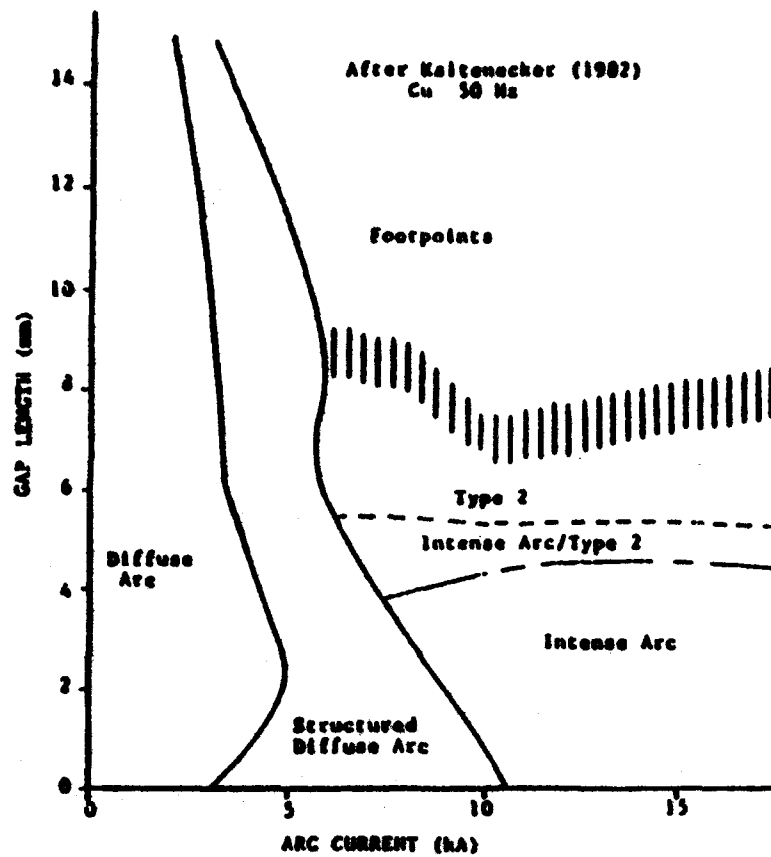


Figure 7 - Anode Discharge Modes as a Function of Current and Gap Length. [Ref. 36]

C. COMPUTER CODE

Rather than using linear approximations to equations (12)-(16), the nonlinear set was used, with initial conditions adjusted in an attempt to produce observed electric fields from probe data. First and second space derivatives of the electric field were used as diagnostic checks to ensure computed output was reasonable. Initial conditions computed from the approximate formulae in Reference 21 were used. The equation set above presents a difficult problem for two reasons, nonlinearity and multiple time constants. The species number density equations, (12) and (13), both contain a nonlinear term, each with a time constant of its own. In addition, the electric field equation, (14), adds a possible third time constant. This constitutes a "stiff" set of equations. Attempts were made to solve the set with the data discussed above, using Gear's method of backward differentiation, in hopes that the variables would change slowly enough with each iteration to render a convergent iterative process. As described in Reference 39, if some reactions are slow and others fast among a set of coupled equations, the fast ones will control the stability of the method. This is addressed in the DGEAR program available from the International Mathematical & Statistical Library (IMSL). The latter software contains an Adams predictor-corrector method, as well as Gear's method, which is well known for its success at solving stiff equation sets. The DGEAR software allows for a choice of functional or chord iteration methods, as well as a choice of Jacobian matrices. A more detailed discussion of this software can be found in Reference 39 and in the IMSL library. [Ref. 39]

D. COMPUTATIONAL RESULTS

Numerous computer runs were completed using the initial conditions taken from Reference 21. In addition, data for the ionization coefficient ν , Figure 8, was taken from References 40 and 41.

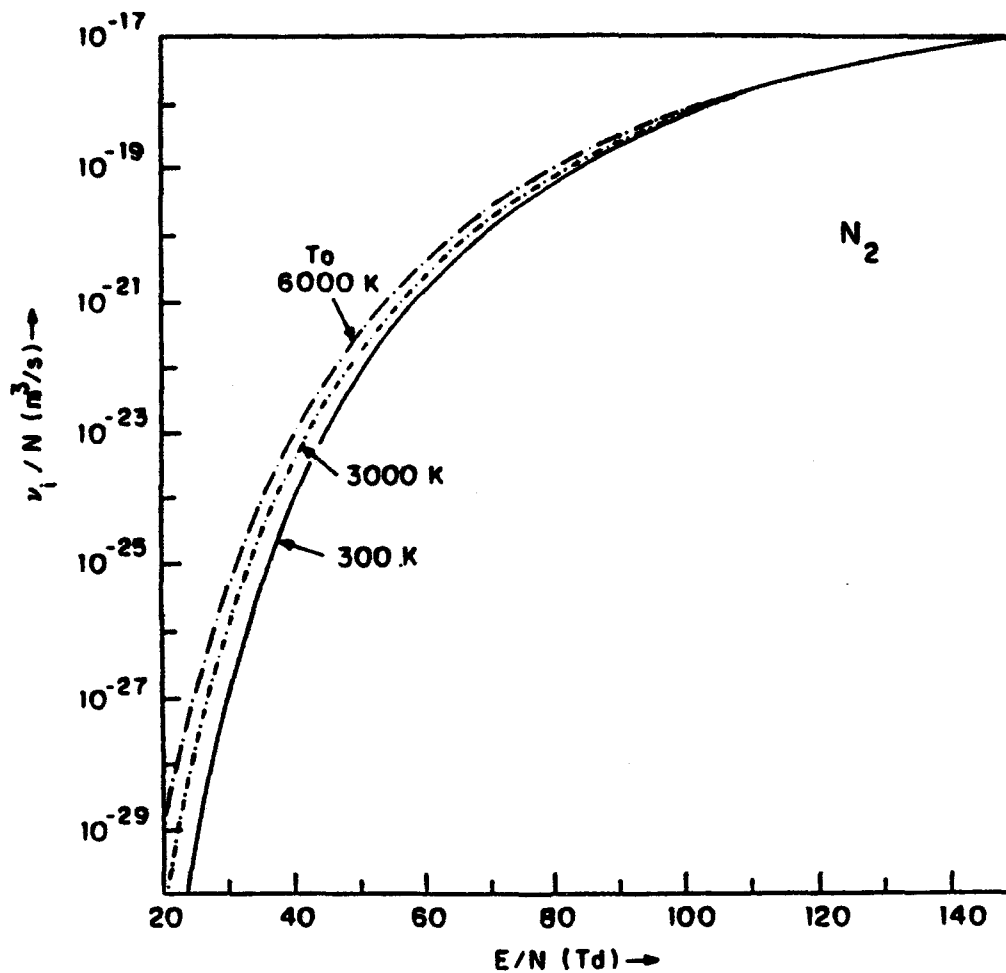


Figure 8. Ionization Coefficient ν as a Function of E/N for Nitrogen for Various Vibrational Temperatures (Refs. 40,41).

Various combinations of initial conditions and ionization coefficient were used. As mentioned above, the electric field and its space derivatives were used as

diagnostic/reasonability checks on the output. Individual, as well as multiple computer runs were attempted to model the sheath region. Nonlinearities in the equation set are clearly seen in Figure 9. The ion number density does not reach that of the electrons, and the latter population growth rate continues to grow without bound. The shape of the electron population curve is very sensitive to its initial value. As shown in Figure 9, the latter population has too high a growth rate when compared to the ion population, and the latter does not "catch up". Increasing the initial value of n_e flattens out this curve to a reasonable shape. Above an initial value of approximately 0.06, however, the plot of n_e "dips" after a certain distance and then continues to increase as expected. This gives an approximate upper value for this initial value. To avoid instabilities like this, small "slices" were taken of the output after a small number of integration steps and multiple runs were used to form a "cut and paste" plot of the region. When a reasonable plot shape was produced, the value of ionization coefficient was varied in the "slices" to attempt to produce the required end values for electric field and species population. Both multiple and equilibrium values for the ionization coefficient were used. When the data showed signs of instability and failure to follow the required forms of Figure 4, a "slice" was made in the data stream, and the data points from this point used to start a new computer run. This approach was taken in the hope of avoiding singularities in the integration from anode surface to ambipolar region. In addition to the diagnostic checks shown in Figure 4, an additional data check is provided by the transition from the sheath to the ambipolar region.

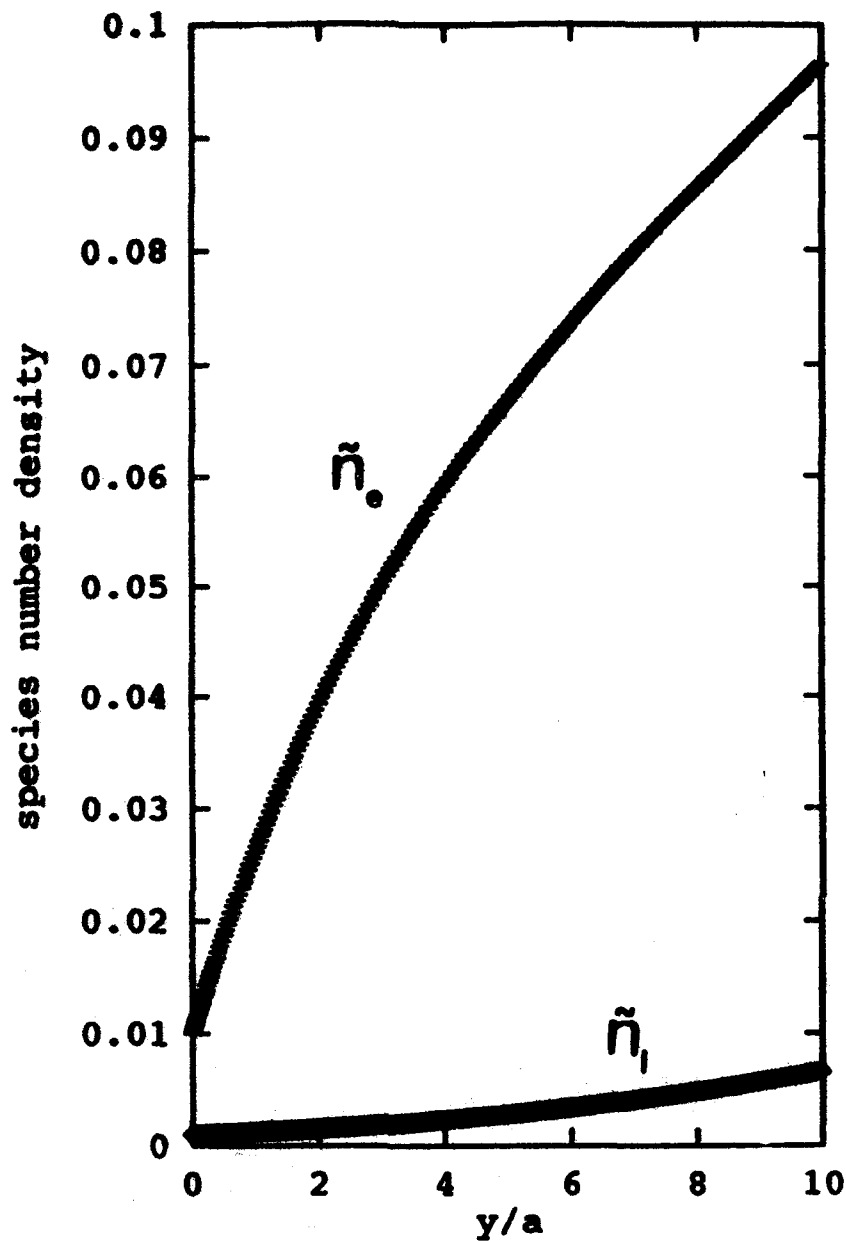


Figure 9. Species Number Density plots for Individual Computer Run, Showing Divergent Tracks for Ion and Electron Populations, and Effect of Nonlinearity.

As shown in Figure 5, the species number densities are equivalent in this region, as are their change rate. Thus, setting Equations (12) and (15) equal to each other and solving for \tilde{n} yields a value of 0.5 in the ambipolar region. As indicated in Figures

10-11, the output produces the desired plot slopes for electric field and species number density. However, the number density plots cross long before approaching the required value of 0.5. In addition, neither electric field nor species number density approaches an equilibrium value or shows sign of levelling off. Apparently, the multiple time constants and nonlinear portions of the number density equations combine to create a seemingly intractable system. Solutions for this system may be possible for specific, individual initial condition sets, but the problem does not appear amenable to this approach in general. A one-dimensional system such as this may be better described through the approach of boundary layer theory or nonlinear dynamics and chaos. Given the effort and difficulty involved in the latter, a one-dimensional approach such as that modelled above does not appear useful. A combination of one- and two-dimensional modelling would appear to be more useful, as discussed in Reference 14. A one-dimensional model may be useful, but only in an approximation approach, with a shaped electric field, such as that used in Reference 21.

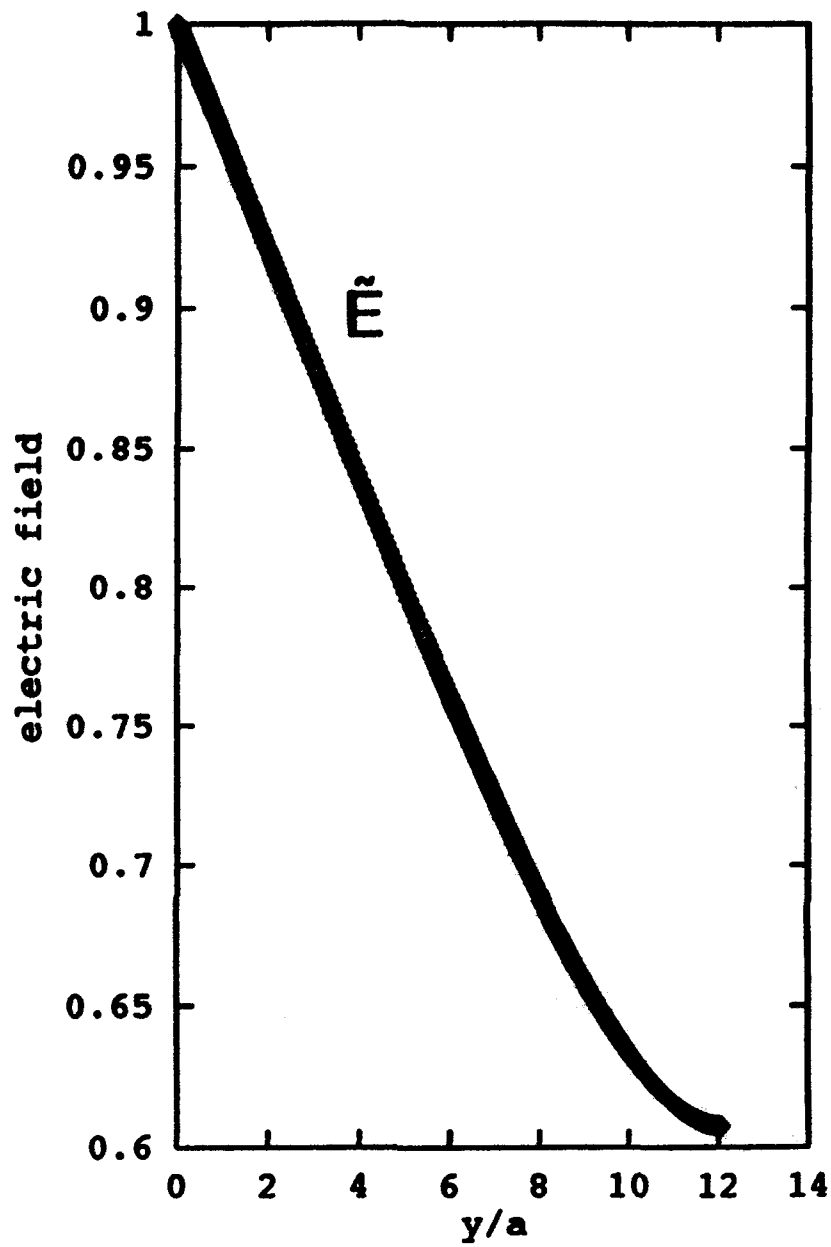


Figure 10. Electric Field as a Function of \bar{y} , Distance From Anode, Using Equations (12)-(16).

ionization (with some help from the tail of the Maxwellian distribution of electron energies), what results is a breakdown voltage appreciably below the ionization potential. This then could be an explanation for the low voltage breakdown observations [Ref. 42]. Clearly, gases with low ionization potentials and lots of atomic electron energy levels are preferred (such as cesium and barium) but low-voltage breakdown has been observed with most gases.

The increase of the anode fall voltage above the ionization potential has been related to the electron Hall parameter, since a reduction of this parameter decreases that voltage and corresponding losses. Control of the local magnetic field through the use of an array of permanent magnets as well as implementation of transpiration cooling (which increases the electron collision frequency) have both yielded some encouraging results. Because the anode fall also scales up with J^2/\dot{m} , it is conceivable that current inhomogeneities and plasma instabilities which are reflected in this parameter are in the picture as well. [Ref. 44]

In summary, any possible reduction of the anode fall voltage will hinge on a thorough understanding of the anode region, with its associated sheath and ambipolar regions, where electron temperature effects, ionization effects, and magnetic field effects play a pivotal role. If transpiration cooling is present, then additional phenomena of fluid-dynamic nature may come into play. Experimental observations with atmospheric discharges indicate the possible presence of convective effects at the anode. [Ref. 45]

IV. TRANSPIRATION COOLING

Transpiration cooling of the anode has often been promoted as an attractive means of recovering a large portion of the power deposited there. Additionally, the onset of melting may be minimized or even avoided by active anode cooling. Rich, et.al., related high anode temperatures to anode spotting [Ref. 37]. Similarly, Park and Choi showed that low thermal diffusion leads to erosion and, consequently, anode damage [Ref. 46]. Active anode cooling via transpiration is one means of ensuring high thermal diffusion and extending anode lifetime. Early work by Schoeck, et. al., [Ref. 47] showed that up to 80% of the energy deposited in the anode is recoverable via transpiration cooling. While this study used non-convective, high-intensity argon arcs, it is reasonable to assume that this effect would apply in MPD arcs using other propellants. Although this cooling method has not been studied for incorporation in plasma thrusters for some time, it has been recently considered as a means of cooling the fuselage of the National Aerospace Plane (NASP). Plasma thruster designs could undoubtedly gain from this database, and due consideration should be given to this cooling approach for the anode.

For a given mass transfer flow rate, the heat flux reduction to a surface is inversely proportional to the molecular weight of the injected gas. Use of the propellant as coolant as well as fuel would eliminate the need for additional tankage and pumps, simplifying the design considerably. Lithium has been considered to be

the propellant of choice, primarily because of its low molecular weight, its favorable ionization potential, and its low-volume tankage properties. It has a relatively low first ionization potential of 5.4 eV and a high second ionization potential of 75.6 eV. This single ionization potential range of over 70 eV compares to approximately 20 eV for Cesium and 27 eV for Potassium [Ref. 48]. This provides a broad temperature range within which only single ionization will occur. Large temperatures must be reached within the gas before double ionization occurs. As the gas temperature is increased several thousand degrees Kelvin, it undergoes ionization and disassociation. Thermal energy deposited can be recovered through nozzle expansion at the exit. However, residence time of the gas is not long enough to ensure recombination. Thus, the energy invested in ionization and disassociation will be lost. [Ref. 49] Lithium has been shown to produce specific impulse figures in excess of 7,000 seconds at 70% efficiency in steady-state thrusters, [Ref. 50] whereas all other propellants have been limited to less than 3,000 seconds specific impulse at less than 40% efficiency [Ref. 6]. Subramaniam has concluded that:

...regenerative cooling of anodes (at the specific impulse values in the MPD regime) is possible only with hydrogen or with alkali-metal propellants, notably lithium. In the latter case, the ideal anode operating mode would be evaporation and ionization of the propellant on the porous or wetted anode surface, resulting in increased ion current fraction, reduced anode voltage fall and utilization of part of the anode loss energy [Ref. 51].

Liquid coolants, as well as reducing storage requirements, offer the advantage of providing latent heat of vaporization for energy disposal. However, design problems can occur if the liquid is allowed to vaporize within the porous structure. Problems

arise due to the abrupt increase in pressure gradient as the coolant vaporizes. Since coolant flow generally have three-dimensional characteristics, the flow will be diverted around the vapor bubbles and hot spots often develop. The technical practicality of using molten lithium to cool a porous tungsten anode would seem to be beyond current technology. On the other hand, the products of decomposition of hydrazine (gaseous hydrogen and ammonia) have proven to be efficient and practical coolants [Ref. 52].

Given the performance figures above, using an auxiliary coolant gas even with high molecular weight (e.g., NH_3 , N_2 , CH_4 , etc.) which could serve as a propellant once released from a porous hot tungsten anode surface would seem to more practical, vice dealing with molten lithium. Experimental studies would be needed to compare the approaches. Kuriki and Suzuki performed experiments with a quasi-steady MPD thruster to study the effect of anode gas injection (Argon). At high currents of up to 10 kA, increases in thrust, specific impulse, and flow discharge stability were observed [Ref. 53].

There is some question as to the likelihood of current constriction resulting from anode gas injection. In such a case, swirling or circulating the propellant gas would help to move any footpoints that developed around the anode surface and prevent them from becoming fully-developed spots. Additionally, an applied magnetic field could serve to circulate the footpoints as well. The unique advantage of transpiration cooling hinges on providing effective anode cooling while supplying

hot propellant, but the real benefit will depend on how small the amount of coolant required really will be.

Transpiration cooling has proven to be as desirable as it is challenging. It is complicated to implement, with associated reliability problems and difficulty of analytical predictions. While the production of thicker boundary layers is largely ineffective against the electron flux heating, the cooling itself is most efficient and a substantial fraction of the energy transferred to the anode is recoverable. The arguments of Chapter Three indicate that a reduction of the electron temperature in the anode would have the desirable effect of reducing the initial current spotting which can be conjectured to be the path that leads to anode arc spots. This electron temperature reduction can be done most effectively by polyatomic gases (which have a high δ -loss factor) emanating from the anode surface [Ref. 54].

The arguments relating to transpiration cooling might be summarized as follows:

Favorable Outcomes

- No separate cooling mechanism for anode required,
- Adds "hot" propellant to exhaust "recovering" most of the electrical power loss to the anode,
- Quenches T_e , thus likely to postpone anode spotting and reduce the heating associated with the electron thermal energy ($5kT_e/2e$),
- Reduces bulk convective heating,
- Reduces the local electron Hall parameter by increasing the collision frequency,

Favorable Outcomes (cont'd.)

- Allows for some radiation cooling from the hot tungsten surface (about 120 watts/cm² at 2800°K [Ref. 51]).
- Hydrogen/ammonia gases flowing through hot porous (sintered) tungsten represent a compatible, proven technology.

Unfavorable Outcomes

- May decrease the electrical conductivity in the anode region,
- May destabilize the ionization processes in the sheath and bring about significant fluctuations in the current,
- Disrupts "cathode jet" in front of the anode with unpredictable consequences,
- Introduces propellant which may not be hot enough, not ionized enough, or not in the proper place for $\vec{j} \times \vec{B}$ acceleration,
- Transpiration cooling through a porous (tungsten) anode is a difficult design problem.

V. CONCLUSIONS AND RECOMMENDATIONS

Plasma thrusters offer distinct advantages in terms of payload delivered for interplanetary missions, as well as for orbital transfer. A recent comparison completed by Choueiri, Kelly, and Jahn shows a mass savings of 65 tons for an orbital transfer from low Earth orbit to geosynchronous Earth orbit using a quasisteady MPD thruster as opposed to an advanced chemical thruster.⁶ This superior performance comes at the expense of low thrust-to-weight ratio and long transit time. However, given the large cargo/logistic requirements of a manned interplanetary mission, delivery of payload must be maximized. Thus, further work to characterize more fully thruster behavior and anode contributions in particular are certainly warranted. [Ref. 55]

The "cut-and-paste" method used to generate Figures 10 and 11 is not of practical use as a modelling method, due to the large effort involved. It did produce the expected electric field and species number and current density plots near the anode, but failed to produce the entire sheath out to the ambipolar region. The nonlinearity of the equation set led to a quickly deteriorating solution. A more practical approach using nonlinear dynamics and/or chaos must be developed to model the sheath numerically.

⁶This assumes a specific impulse of 2,000 seconds, 600 kW of input power, and a 270-day transit time.

Depending on the propellant mass fraction used for cooling, the transpiration scheme discussed above presents some rather unique advantages. A hot anode which uses only a small amount of propellant for cooling need not be penalized for any lost thrust. If in addition, we increase anode lifetime by delaying the formation of anode arc spots, then the scheme is all the more desirable. A decrease of the electron temperature in the vicinity of the anode may bring about a more homogeneous flow of current and a reduction in the heating effect associated with the high electron kinetic energy. Recovery of the heat deposited at the anode would be most important if the propellant fraction is high. In such case, nozzle expansion of the hot-propellant/coolant-gas might be implemented.

Means of limiting anode losses through decreasing anode fall voltages were discussed, including the control of the local Hall parameter and the implementation of thermionic arc breakdown. The electrical conductivity (of a nonreacting plasma) could possibly decrease as a result of transpiration cooling and this might increase the anode fall voltage.

Additional work needs to be done in the following areas:

- Investigate effectiveness of nonlinear dynamics and chaos in solving sheath equation set,
- Incorporate adequate one- or two-dimensional sheath modelling in quasisteady MPD numerical codes,

- Investigate the role that fluid dynamic effects play in MPD thruster anode discharges,
- Investigate the effect of transpiration cooling on current and plasma stability, as well as on thruster performance and lifetime,
- Determine effectiveness of transpiration cooling's increase of the collision frequency parameter,
- Compare performance of gaseous propellant/coolants versus hybrid designs with lithium propellant/gaseous coolant,
- Determine if required percentage of propellant gas as coolant is practical (e.g., less than 10%),
- Investigate effect of surface imperfections as focal points for current constrictions and as precursors to anode spotting.

APPENDIX A

The following software includes the calling program, SHEATH, its two subroutines, FCNJ and YDOT, and the DGEAR integrator. The latter is quite extensive in length and includes ten subroutines, including the following: DGRST, DGRCS, DGRPS, DGRIN, LUDATF, LUELMF, LEQT1B, UERTST, UGETIO, and USPKD. A detailed discussion may be found in IMSL literature or Reference 39.

```

*****
      Program Sheath                                000010
C                                          000020
C-----Calling program for DGEAR integrator. Initial conditions are      000030
C input via READ statements and keyboard entry. Output is to data         000040
C files via the DGRST subroutine. Diagnostic check of output via          000050
C Figure 4 printed to data file from DGRST subroutine. Consult            000060
C DGEAR comments for variable descriptions not listed below.              000061
C-----
      REAL E,K,EPS,TI,EF,EFINF,DI,DE,NUINF,C1,K1,A      000070
      INTEGER N,METH,MITER,INDEX,IWK(1),IER,STEP      000080
      REAL*8 X,H,Y(5),XEND,TOL,WK                     000090
      EXTERNAL YDOT,FCNJ,DGEAR                         000100
      COMMON/CONST/E,K,EPS,TI,EF,EFINF,NINF,DI,DE,VINF,C1,K1,A 000110
C                                          000120
C-----Constants                                000121
C C1 and K1 are constants describing the ionization coefficient.           000122
C They are taken from the data plotted in Figure 8. The                  000123
C coefficient is equal to the nondimensionalized electric potential       000124
C raised to the K1 power and then multiplied by C1.                      000125
C In this way, the ionization coefficient is allowed to vary in          000126
C proportion to the strength of the electric potential.                  000127
C-----
      WRITE(*,*)'Input value for C1 (format 6E3):'    000128
      READ(*,*)C1                                     000129
      WRITE(*,*)C1                                    000130
      WRITE(*,*)'Input value for K1 (format 6E3):'    000131
      READ(*,*)K1                                     000132
      WRITE(*,*)K1                                    000133
      WRITE(*,*)K1                                    000134
C Initial conditions for species number density, electric potential       000135
C and species current density are now input (ni,ne,E,je,ji).              000136
C-----
      WRITE(*,*)'Input values for y(1) through y(5) (format 5(6E3)):'    000137
      READ(*,*)y(1),y(2),y(3),y(4),y(5)              000138
      WRITE(*,*)y(1),y(2),y(3),y(4),y(5)             000139
C Following constants are for plasma described in Reference 21            000140
C (6,000 K, Init E=20,000 V/m, Final E=1,200 V/m)                          000141
C                                          000142
      E=1.6E-19                                         000143
      K=1.38E-23                                        000150
      EPS=8.854E-12                                    000160
      TI=6E3                                           000170
      EF=2E5                                           000180
      EFINF=1.2E4                                       000190
      DI=1.724E-4                                       000200
      DE=1.724E-1                                       000210
      VIO = 2.E6                                        000215
      VINF = 4.93E-7                                    000220
C                                          000230

```

```

C      A is plasma characteristic length which shows potential drop.          000240
C      A = ((EPS*EF)/(E*NINF)) = 1.107E-6
A = 1.107E-5          000250
X = 0.01              000270
XEND = 10.           000280
H = 1e-6             000290
TOL = 1E-6          000300
METH = 2             000305
MITER = 1           000310
INDEX = 1           000320
N=5                  000330
IWK(1) = 5          000340
WK = 18000.         000350
IER = 0             000360
OPEN(UNIT=8, FILE='SHEATH.DAT', STATUS='UNKNOWN') 000370
CALL DGEAR2(N, YDOT, FCNJ, X, H, Y, XEND, TOL, METH, MITER, INDEX, IWK, WK,
+IER, STEP)         000380
DO 3 I=0, N         000390
DO 2 J=0, 100      000400
WRITE(*,*) J, Y(I) 000420
WRITE(8,1) J, Y(I) 000430
1  FORMAT(T2, F5.1, 5(5X, D9.2)) 000440
2  CONTINUE        000450
3  CONTINUE        000460
WRITE(*,*) 'Total Steps = ', STEP, 'Final Step Size = ', H,
+'Error Code = ', IER 000480
CLOSE(UNIT=8)      000490
STOP               000500
END               000510
C*****
C DUMMY SUBROUTINE FCNJ
C*****
SUBROUTINE FCNJ(N, X, Y, PD)          1
INTEGER N                            2
REAL Y(N), PD(N, N), X               3
RETURN                                4
END                                    5
C*****
C SUBROUTINE YDOT
C*****
SUBROUTINE YDOT(N, X, Y, YPRIME, eprime, eprime2)
REAL*8 X, Y(5), YPRIME(5), NUI, eprime, eprime2
REAL E, K, EPS, TI, EF, EFINF, NINF, DI, DE, VINP, C1, K1, A, B1, B2, B3, B4
COMMON/CONST/E, K, EPS, TI, EF, EFINF, NINF, DI, DE, VIO, VINP, C1, K1, A
VI = C1 * (Y(3)**K1)
VIT = VI / VIO
C      Following constants are the bracketed values in Equations 12-16.
C      A is left as a variable.
C-----
C      B1 = ((E*EPS)/(K*TI)) * A
B1 = 3.86E5 * A
C      B2 = ((E*EFINF)/(K*TI)) * A
B2 = 2.32E4 * A
C      B3 = ((E*NINF)/(EF*EPS)) * A
B3 = 9.04E5 * A
C      B4 = ((VINP*K*TI)/(E*DE*EFINF)) * A
B4 = 2.62E-21 * A
C      Alpha = 2-body recombination coefficient (fm. Laser Kinetics
C      Handbook (AFWL-TR-74-216, 1974)) (cm3/sec)
Alpha = 9.e-8

```

```

C-----
C FIVE FIRST ORDER EQUATIONS - Equations 12-16
C-----
C      Ni
C      YPRIME(1) = (B * Y(1) * Y(3)) - Y(5)
C      No
C      YPRIME(2) = -(B * Y(2) * Y(3)) + Y(4)
C      E
C      YPRIME(3) = B3 * (Y(1) - Y(2))
C      je
C      YPRIME(4) = -B4 * Y(2) * (VIT - (ALPHA * Y(1)))
C      ji
C      YPRIME(5) = B4 * Y(2) * (VIT - (ALPHA * Y(1)))
C
C---Diagnostic Check of first,second derivatives-----
C
C      eprime = y(1) - y(2)
C      eprime2 = yprime(1) - yprime(2)
C
C      RETURN
C      END

```

```

C   IMSL ROUTINE NAME   - DGEAR                               DGEA0010
C                                                                DGEA0020
C--modified to return # of steps via variable "step" in subroutine call +
C                                                                DGEA0040
C   COMPUTER           - IBM/DOUBLE                          DGEA0050
C                                                                DGEA0060
C   LATEST REVISION    - NOVEMBER 1, 1984                   DGEA0070
C                                                                DGEA0080
C   PURPOSE            - DIFFERENTIAL EQUATION SOLVER - VARIABLE ORDER DGEA0090
C                       ADAMS PREDICTOR CORRECTOR METHOD OR   DGEA0100
C                       GEARS METHOD                          DGEA0110
C                                                                DGEA0120
C   USAGE              - CALL DGEAR (N,FCN,FCNJ,X,H,Y,XEND,TOL,METH, DGEA0130
C                       MITER,INDEX,IWK,WK,IER)              DGEA0140
C                                                                DGEA0150
C   ARGUMENTS          N   - INPUT NUMBER OF FIRST-ORDER DIFFERENTIAL DGEA0160
C                       EQUATIONS.                            DGEA0170
C                       FCN - NAME OF SUBROUTINE FOR EVALUATING FUNCTIONS. DGEA0180
C                           (INPUT)                           DGEA0190
C                           THE SUBROUTINE ITSELF MUST ALSO BE PROVIDED DGEA0200
C                           BY THE USER AND IT SHOULD BE OF THE DGEA0210
C                           FOLLOWING FORM                     DGEA0220
C                           SUBROUTINE FCN (N,X,Y,YPRIME)      DGEA0230
C                           REAL X,Y(N),YPRIME(N)             DGEA0240
C                           .                                   DGEA0250
C                           .                                   DGEA0260
C                           .                                   DGEA0270
C                           FCN SHOULD EVALUATE YPRIME(1),...,YPRIME(N) DGEA0280
C                           GIVEN N,X, AND Y(1),...,Y(N). YPRIME(I) DGEA0290
C                           IS THE FIRST DERIVATIVE OF Y(I) WITH DGEA0300
C                           RESPECT TO X.                      DGEA0310
C                           FCN MUST APPEAR IN AN EXTERNAL STATEMENT IN DGEA0320
C                           THE CALLING PROGRAM AND N,X,Y(1),...,Y(N) DGEA0330
C                           MUST NOT BE ALTERED BY FCN.       DGEA0340
C                       FCNJ - NAME OF THE SUBROUTINE FOR COMPUTING THE DGEA0350
C                           JACOBIAN MATRIX OF PARTIAL DERIVATIVES. DGEA0360
C                           (INPUT)                            DGEA0370
C                           THE SUBROUTINE ITSELF MUST ALSO BE PROVIDED DGEA0380
C                           BY THE USER.                      DGEA0390
C                           IF MITER=1 IT SHOULD BE OF THE FOLLOWING DGEA0400
C                           FORM                                DGEA0410
C                           SUBROUTINE FCNJ (N,X,Y,PD)         DGEA0420
C                           REAL X,Y(N),PD(N,N)               DGEA0430
C                           .                                   DGEA0440
C                           .                                   DGEA0450
C                           FCNJ MUST EVALUATE PD(I,J), THE PARTIAL DGEA0460
C                           DERIVATIVE OF YPRIME(I) WITH RESPECT TO DGEA0470
C                           Y(J), FOR I=1,N AND J=1,N.        DGEA0480
C                           IF MITER= -1 IT SHOULD BE OF THE FOLLOWING DGEA0490
C                           FORM                                DGEA0500
C                           SUBROUTINE FCNJ (N,X,Y,PD)         DGEA0510
C                           REAL X,Y(N),PD(1)                 DGEA0520
C                           .                                   DGEA0530
C                           .                                   DGEA0540
C                           FCNJ MUST EVALUATE PD IN BAND STORAGE MODE. DGEA0550
C                           THAT IS, PD(N*(J-I+NLC)+I) IS THE PARTIAL DGEA0560
C                           DERIVATIVE OF YPRIME(I) WITH RESPECT TO DGEA0570
C                           Y(J). NLC IS THE NUMBER OF LOWER DGEA0580
C                           CODIAGONALS FOR THE BAND MATRIX. DGEA0590
C                           FCNJ MUST APPEAR IN AN EXTERNAL STATEMENT INDGEA0600
C                           THE CALLING PROGRAM AND N,X,Y(1),...,Y(N) DGEA0610

```


	MITER = 2, IMPLIES THAT THE CHORD METHOD	DGEA1240
	IS USED WITH THE JACOBIAN CALCULATED	DGEA1250
	INTERNALLY BY FINITE DIFFERENCES.	DGEA1260
	A DUMMY FCNJ CAN BE USED.	DGEA1270
	MITER = 3, IMPLIES THAT THE CHORD METHOD	DGEA1280
	IS USED WITH THE JACOBIAN REPLACED BY	DGEA1290
	A DIAGONAL APPROXIMATION BASED ON A	DGEA1300
	DIRECTIONAL DERIVATIVE.	DGEA1310
	A DUMMY FCNJ CAN BE USED.	DGEA1320
	MITER = -1 OR -2, IMPLIES USE THE SAME	DGEA1330
	METHOD AS FOR MITER= 1 OR 2, RESPECTIVELY,	DGEA1340
	BUT USING A Banded JACOBIAN MATRIX. IN	DGEA1350
	THESE TWO CASES BANDWIDTH INFORMATION	DGEA1360
	MUST BE PASSED TO DGEAR THROUGH THE	DGEA1370
	COMMON BLOCK	DGEA1380
	COMMON /DBAND/ NLC,NUC	DGEA1390
	WHERE NLC=NUMBER OF LOWER CODIAGONALS	DGEA1400
	NUC=NUMBER OF UPPER CODIAGONALS	DGEA1410
INDEX	- INPUT AND OUTPUT PARAMETER USED TO INDICATE	DGEA1420
	THE TYPE OF CALL TO THE SUBROUTINE. ON	DGEA1430
	OUTPUT INDEX IS RESET TO 0 IF INTEGRATION	DGEA1440
	WAS SUCCESSFUL. OTHERWISE, THE VALUE OF	DGEA1450
	INDEX IS UNCHANGED.	DGEA1460
	ON INPUT, INDEX = 1, IMPLIES THAT THIS IS THE	DGEA1470
	FIRST CALL FOR THIS PROBLEM.	DGEA1480
	ON INPUT, INDEX = 0, IMPLIES THAT THIS IS NOT	DGEA1490
	THE FIRST CALL FOR THIS PROBLEM.	DGEA1500
	ON INPUT, INDEX = -1, IMPLIES THAT THIS IS NOT	DGEA1510
	THE FIRST CALL FOR THIS PROBLEM, AND THE	DGEA1520
	USER HAS RESET TOL.	DGEA1530
	ON INPUT, INDEX = 2, IMPLIES THAT THIS IS NOT	DGEA1540
	THE FIRST CALL FOR THIS PROBLEM. INTEGRATION	DGEA1550
	IS TO CONTINUE AND XEND IS TO BE HIT EXACTLY	DGEA1560
	(NO INTERPOLATION IS DONE). THIS VALUE OF	DGEA1570
	INDEX ASSUMES THAT XEND IS BEYOND THE	DGEA1580
	CURRENT VALUE OF X.	DGEA1590
	ON INPUT, INDEX = 3, IMPLIES THAT THIS IS NOT	DGEA1600
	THE FIRST CALL FOR THIS PROBLEM. INTEGRATION	DGEA1610
	IS TO CONTINUE AND CONTROL IS TO BE RETURNED	DGEA1620
	TO THE CALLING PROGRAM AFTER ONE STEP. XEND	DGEA1630
	IS IGNORED.	DGEA1640
IWK	- INTEGER WORK VECTOR OF LENGTH N. USED ONLY IF	DGEA1650
	MITER = 1 OR 2	DGEA1660
WK	- REAL WORK VECTOR OF LENGTH 4*N+NMETH+NMITER.	DGEA1670
	THE VALUE OF NMETH DEPENDS ON THE VALUE OF	DGEA1680
	METH.	DGEA1690
	IF METH IS EQUAL TO 1,	DGEA1700
	NMETH IS EQUAL TO N*13.	DGEA1710
	IF METH IS EQUAL TO 2,	DGEA1720
	NMETH IS EQUAL TO N*6.	DGEA1730
	THE VALUE OF NMITER DEPENDS ON THE VALUE OF	DGEA1740
	MITER.	DGEA1750
	IF MITER IS EQUAL TO 1 OR 2,	DGEA1760
	NMITER IS EQUAL TO N*(N+1)	DGEA1770
	IF MITER IS EQUAL TO -1 OR -2,	DGEA1780
	NMITER IS EQUAL TO (2*NLC+NUC+3)*N	DGEA1790
	WHERE NLC=NUMBER OF LOWER CODIAGONALS	DGEA1800
	NUC=NUMBER OF UPPER CODIAGONALS	DGEA1810
	IF MITER IS EQUAL TO 3,	DGEA1820
	NMITER IS EQUAL TO N.	DGEA1830
	IF MITER IS EQUAL TO 0,	DGEA1840
	NMITER IS EQUAL TO 1.	DGEA1850

C	25 IF ((T+HH).EQ.T) KER = 33	DGEA4950
	write(*,*) 'error code = ',ker	DGEA4960
C	30 NN = NO	+ DGEA4970
	step = step + 1	DGEA4980
	write(*,*) 'step = ',step	+ +
	CALL DGRST (FCN,FCNJ,WK(NY+1),WK,WK(NERROR+1),WK(NSAVE1+1),	DGEA4990
	1 WK(NSAVE2+1),WK(NPW+1),WK(NEQUIL+1),IWK,NN,step)	+ DGEA5010
C	RGO = 1-KFLAG	DGEA5020
	GO TO (35,55,70,80), KGO	DGEA5030
C	35 CONTINUE	KFLAG = 0, -1, -2, -3 DGEA5040
C		DGEA5050
C		DGEA5060
C		DGEA5070
C		DGEA5080
C		DGEA5090
C		DGEA5100
C		DGEA5110
C		DGEA5120
C		DGEA5130
C		DGEA5140
C		DGEA5150
C		DGEA5160
C		DGEA5170
C		DGEA5180
C		DGEA5190
C		DGEA5200
C		DGEA5210
C		DGEA5220
C		DGEA5230
C		DGEA5240
C		DGEA5250
C		DGEA5260
C		DGEA5270
C		DGEA5280
C		DGEA5290
C		DGEA5300
	D = 0.D0	DGEA5310
	DO 40 I=1,N	DGEA5320
	AYI = DABS(WK(NY+I))	DGEA5330
	WK(I) = DMAX1(WK(I),AYI)	DGEA5340
40	D = D+(AYI/WK(I))**2	DGEA5350
	D = D*(UROUND/TOL)**2	DGEA5360
	DN = N	DGEA5370
	IF (D.GT.DN) GO TO 75	DGEA5380
	IF (INDEX.EQ.3) GO TO 95	DGEA5390
	IF (INDEX.EQ.2) GO TO 50	DGEA4000
45	IF ((T-XEND)*HH.LT.0.D0) GO TO 25	DGEA4100
	NN = NO	DGEA4200
	CALL DGRIN (XEND,WK(NY+1),NN,Y)	DGEA4300
	X = XEND	DGEA4400
	GO TO 105	DGEA4500
50	IF (((T+HH)-XEND)*HH.LE.0.D0) GO TO 25	DGEA4600
	IF (DABS(T-XEND).LE.UROUND*DMAX1(10.D0*DABS(T),HMAX)) GO TO 95	DGEA4700
	IF ((T-XEND)*HH.GE.0.D0) GO TO 95	DGEA4800
	HH = (XEND-T)*(1.D0-4.D0*UROUND)	DGEA4900
	JSTART = -1	DGEA5000
	GO TO 25	DGEA5100
C		DGEA5510
C		DGEA5520
C		DGEA5530
	ON AN ERROR RETURN FROM INTEGRATOR,	
	AN IMMEDIATE RETURN OCCURS IF	
	KFLAG = -2, AND RECOVERY ATTEMPTS	

C		ARE MADE OTHERWISE. TO RECOVER, HH	DGRA5540
C		AND HMIN ARE REDUCED BY A FACTOR	DGRA5550
C		OF .1 UP TO 10 TIMES BEFORE GIVING	DGRA5560
C		UP.	DGRA5570
	55	JER = 66	DGRA5580
	60	IF (NHCUT.EQ.10) GO TO 65	DGRA5590
		NHCUT = NHCUT+1	DGRA5600
		HMIN = HMIN*.1D0	DGRA5610
		HH = HH*.1D0	DGRA5620
		JSTART = -1	DGRA5630
		GO TO 25	DGRA5640
C			DGRA5650
	65	IF (JER.EQ.66) JER = 132	DGRA5660
		IF (JER.EQ.67) JER = 133	DGRA5670
		GO TO 95	DGRA5680
C			DGRA5690
	70	JER = 134	DGRA5700
		GO TO 95	DGRA5710
C			DGRA5720
	75	JER = 134	DGRA5730
		KFLAG = -2	DGRA5740
		GO TO 95	DGRA5750
C			DGRA5760
	80	JER = 67	DGRA5770
		GO TO 60	DGRA5780
C			DGRA5790
	85	JER = 135	DGRA5800
		GO TO 110	DGRA5810
C			DGRA5820
	90	JER = 136	DGRA5830
		NN = NO	DGRA5840
		CALL DGRIN (XEND,WK(NY+1),NN,Y)	DGRA5850
		X = XEND	DGRA5860
		GO TO 110	DGRA5870
C			DGRA5880
	95	X = T	DGRA5890
		DO 100 I=1,N	DGRA5900
	100	Y(I) = WK(NY+I)	DGRA5910
	105	IF (JER.LT.128) INDEX = KFLAG	DGRA5920
		TOUTP = X	DGRA5930
		IF (KFLAG.EQ.0) H = HUSED	DGRA5940
		IF (KFLAG.NE.0) H = HH	DGRA5950
	110	IER = MAX0(KER,JER)	DGRA5960
	9000	CONTINUE	DGRA5970
		IF (KER.NE.0.AND.JER.LT.128) CALL UERTST (KER,6HDGEAR)	DGRA5980
		IF (JER.NE.0) CALL UERTST (JER,6HDGEAR)	DGRA5990
	9005	RETURN	DGEA6000
		END	DGEA6010


```

C   IMSL ROUTINE NAME   - DGRST                                     DGRS0010
C                                                                DGRS0020
C-modified to print sheath and diagnostic output to files "sheatha.dat" +
C and "diag.dat"                                             +
C   COMPUTER           - IBM/DOUBLE                               DGRS0050
C                                                                DGRS0060
C   LATEST REVISION    - JUNE 1, 1982                           DGRS0070
C                                                                DGRS0080
C   PURPOSE            - NUCLEUS CALLED ONLY BY IMSL SUBROUTINE DGEAR DGRS0090
C                                                                DGRS0100
C   PRECISION/HARDWARE - SINGLE AND DOUBLE/H32                 DGRS0110
C                                                                DGRS0120
C                                                                DGRS0130
C   REQD. IMSL ROUTINES - DGRCS, DGRPS, LUDATF, LUELMF, LEQT1B, UERTST, DGRS0140
C                                                                DGRS0150
C                                                                DGRS0160
C   NOTATION           - INFORMATION ON SPECIAL NOTATION AND    DGRS0170
C                                                                DGRS0180
C                                                                DGRS0190
C                                                                DGRS0200
C                                                                DGRS0210
C                                                                DGRS0220
C   WARRANTY           - IMSL WARRANTS ONLY THAT IMSL TESTING HAS BEEN DGRS0230
C                                                                DGRS0240
C                                                                DGRS0250
C                                                                DGRS0260
C-----DGRS0270
C                                                                DGRS0280
C                                                                DGRS0290
C   SUBROUTINE DGRST (FCN, FCNJ, Y, YMAX, ERROR, SAVE1, SAVE2, PW, EQUIL,
1     IPIV, NO, step)
C                                                                DGRS0310
C                                                                DGRS0320
C                                                                DGRS0330
C                                                                DGRS0350
C                                                                DGRS0360
C                                                                DGRS0370
C                                                                DGRS0380
C                                                                DGRS0390
C                                                                DGRS0400
C                                                                DGRS0410
C                                                                DGRS0420
C                                                                DGRS0430
C                                                                DGRS0440
C                                                                DGRS0460
C                                                                DGRS0470
C                                                                DGRS0480
C                                                                DGRS0490
C                                                                DGRS0500
C                                                                DGRS0510
C                                                                DGRS0520
C                                                                DGRS0530
C                                                                DGRS0540
C                                                                DGRS0550
C                                                                DGRS0560
C                                                                DGRS0570
C                                                                DGRS0580
C                                                                DGRS0590
C                                                                DGRS0600
C   SPECIFICATIONS FOR ARGUMENTS
C   INTEGER             IPIV(1), NO
C   DOUBLE PRECISION    Y(NO,1), YMAX(1), ERROR(1), SAVE1(1), SAVE2(1),
1     PW(1), EQUIL(1), eprime, eprime(2)
C   SPECIFICATIONS FOR LOCAL VARIABLES
C   INTEGER             N, MF, KFLAG, JSTART, NQUSED, NSTEP, NFE, NJE, NSQ,
1     I, METH, MITER, NQ, L, IDOUB, MFOLD, NOLD, IRET, MEO,
2     MIO, IWEVAL, MAXDER, LMAX, IREDO, J, NSTEPJ, J1, J2,
3     M, IER, NEWQ, NPW, NERROR, NSAVE1, NSAVE2, NEQUIL, NY,
4     MITER1, IDUMMY(2), NLC, NUC, NWK, JER
C   REAL                TQ(4)
C   DOUBLE PRECISION    T, H, HMIN, HMAX, EPS, UROUND, HUSED, EL(13), OLDLO,
1     TOLD, RMAX, RC, CRATE, EPSOLD, HOLD, FN, EDN, E, EUP,
2     BND, RH, R1, CON, R, HLO, RO, D, PHLO, PR3, D1, ENQ3, ENQ2,
3     PR2, PR1, ENQ1, EPSJ, DUMMY, tcum
C   EXTERNAL            FCN, FCNJ
C   COMMON /DBAND/      NLC, NUC
C   COMMON /GEAR/      T, H, HMIN, HMAX, EPS, UROUND, EPSJ, HUSED,
1     EL, OLDLO, TOLD, RMAX, RC, CRATE, EPSOLD, HOLD, FN,
2     EDN, E, EUP, BND, RH, R1, R, HLO, RO, D, PHLO, PR3, D1,
3     ENQ3, ENQ2, PR2, PR1, ENQ1, DUMMY, TQ,
4     N, MF, KFLAG, JSTART, NSQ, NQUSED, NSTEP, NFE, NJE,
5     NPW, NERROR, NSAVE1, NSAVE2, NEQUIL, NY,
6     I, METH, MITER, NQ, L, IDOUB, MFOLD, NOLD, IRET, MEO,
7     MIO, IWEVAL, MAXDER, LMAX, IREDO, J, NSTEPJ, J1, J2,
8     M, NEWQ, IDUMMY
C   FIRST EXECUTABLE STATEMENT
C   open(unit=8, file='sheatha.dat', status='unknown')
C   open(unit=9, file='diag.dat', status='unknown')
C   KFLAG = 0
C   TO: D = T
C   THIS ROUTINE PERFORMS ONE STEP OF

```

C
C
C
C
C
C
C
C
C
C

IF (JSTART.GT.0) GO TO 50
IF (JSTART.NE.0) GO TO 10

THE INTEGRATION OF AN INITIAL
VALUE PROBLEM FOR A SYSTEM OF
ORDINARY DIFFERENTIAL EQUATIONS.

ON THE FIRST CALL, THE ORDER IS SET
TO 1 AND THE INITIAL YDOT IS
CALCULATED. RMAX IS THE MAXIMUM
RATIO BY WHICH H CAN BE INCREASED
IN A SINGLE STEP. IT IS INITIALLY
1.E4 TO COMPENSATE FOR THE SMALL
INITIAL H, BUT THEN IS NORMALLY
EQUAL TO 10. IF A FAILURE OCCURS
(IN CORRECTOR CONVERGENCE OR ERROR
TEST), RMAX IS SET AT 2 FOR THE
NEXT INCREASE.

DGRS0610
DGRS0620
DGRS0630
DGRS0640
DGRS0650
DGRS0660
DGRS0670
DGRS0680
DGRS0690
DGRS0700
DGRS0710
DGRS0720
DGRS0730
DGRS0740
DGRS0750
DGRS0760

CALL FCN (N,T,Y,SAVE1,eprime,epsilon2)
DO 5 I=1,N
5 Y(I,2) = H*SAVE1(I)
METH = MF/10
MITER = MF-10*METH
NQ = 1
L = 2
IDOU B = 3
RMAX = 1.D4
RC = 0.D0
CRATE = 1.D0
HOLD = H
MFOLD = MF
NSTEP = 0
NSTEPJ = 0
NFE = 1
NJE = 0
IRET = 3
GO TO 15

+
DGRS0780
DGRS0790
DGRS0800
DGRS0810
DGRS0820
DGRS0830
DGRS0840
DGRS0850
DGRS0860
DGRS0870
DGRS0880
DGRS0890
DGRS0900
DGRS0910
DGRS0920
DGRS0930
DGRS0940
DGRS0950

C
C
C
C
C
C
C
C
C
C
C
C

IF THE CALLER HAS CHANGED METH,
DGRCS IS CALLED TO SET THE
COEFFICIENTS OF THE METHOD. IF THE
CALLER HAS CHANGED N, EPS, OR
METH, THE CONSTANTS E, EDN, EUP,
AND BND MUST BE RESET. E IS A
COMPARISON FOR ERRORS OF THE
CURRENT ORDER NQ. EUP IS TO TEST
FOR INCREASING THE ORDER, EDN FOR
DECREASING THE ORDER. BND IS USED
TO TEST FOR CONVERGENCE OF THE
CORRECTOR ITERATES. IF THE CALLER
HAS CHANGED H, Y MUST BE RESCALED.
IF H OR METH HAS BEEN CHANGED,
IDOU B IS RESET TO L + 1 TO PREVENT
FURTHER CHANGES IN H FOR THAT MANY
STEPS.

DGRS0960
DGRS0970
DGRS0980
DGRS0990
DGRS1000
DGRS1010
DGRS1020
DGRS1030
DGRS1040
DGRS1050
DGRS1060
DGRS1070
DGRS1080
DGRS1090
DGRS1100
DGRS1110
DGRS1120

10 IF (MF.EQ.MFOLD) GO TO 25
MEO = METH
MIO = MITER
METH = MF/10
MITER = MF-10*METH
MFOLD = MF
IF (MITER.NE.MIO) IWEVAL = MITER
IF (METH.EQ.MEO) GO TO 25
IDOU B = L+1
IRET = 1

DGRS1130
DGRS1140
DGRS1150
DGRS1160
DGRS1170
DGRS1180
DGRS1190
DGRS1200
DGRS1210
DGRS1220

15	CALL DGRCS (METH,NQ,EL,TQ,MAXDER)	DGRS1230
	LMAX = MAXDER+1	DGRS1240
	RC = RC*EL(1)/OLDLO	DGRS1250
	OLDLO = EL(1)	DGRS1260
20	FN = N	DGRS1270
	EDN = FN*(TQ(1)*EPS)**2	DGRS1280
	E = FN*(TQ(2)*EPS)**2	DGRS1290
	EUP = FN*(TQ(3)*EPS)**2	DGRS1300
	BND = FN*(TQ(4)*EPS)**2	DGRS1310
	EPSOLD = EPS	DGRS1320
	NOLD = N	DGRS1330
	GO TO (30,35,50), IRET	DGRS1340
25	IF ((EPS.EQ.EPSOLD).AND.(N.EQ.NOLD)) GO TO 30	DGRS1350
	IF (N.EQ.NOLD) IWEVAL = MITER	DGRS1360
	IRET = 1	DGRS1370
	GO TO 20	DGRS1380
30	IF (H.EQ.HOLD) GO TO 50	DGRS1390
	RH = H/HOLD	DGRS1400
	H = HOLD	DGRS1410
	IREDO = 3	DGRS1420
	GO TO 40	DGRS1430
35	RH = DMAX1(RH,HMIN/DABS(H))	DGRS1440
40	RH = DMIN1(RH,HMAX/DABS(H),RMAX)	DGRS1450
	R1 = 1.D0	DGRS1460
	DO 45 J=2,L	DGRS1470
	R1 = R1*RH	DGRS1480
	DO 45 I=1,N	DGRS1490
45	Y(I,J) = Y(I,J)*R1	DGRS1500
	H = H*RH	DGRS1510
	RC = RC*RH	DGRS1520
	IDOUB = L+1	DGRS1530
	IF (IREDO.EQ.0) GO TO 285	DGRS1540
	THIS SECTION COMPUTES THE PREDICTED	DGRS1550
	VALUES BY EFFECTIVELY MULTIPLYING	DGRS1560
	THE Y ARRAY BY THE PASCAL TRIANGLE	DGRS1570
	MATRIX. RC IS THE RATIO OF NEW TO	DGRS1580
	OLD VALUES OF THE COEFFICIENT	DGRS1590
	H*EL(1). WHEN RC DIFFERS FROM 1 BY	DGRS1600
	MORE THAN 30 PERCENT, OR THE	DGRS1610
	CALLER HAS CHANGED MITER, IWEVAL	DGRS1620
	IS SET TO MITER TO FORCE THE	DGRS1630
	PARTIALS TO BE UPDATED, IF	DGRS1640
	PARTIALS ARE USED. IN ANY CASE,	DGRS1650
	THE PARTIALS ARE UPDATED AT LEAST	DGRS1660
	EVERY 20-TH STEP.	DGRS1670
50	IF (DABS(RC-1.D0).GT.0.3D0) IWEVAL = MITER	DGRS1680
	IF (NSTEP.GE.NSTEPJ+20) IWEVAL = MITER	DGRS1690
	T = T+H	DGRS1700
	DO 55 J1=1,NQ	DGRS1710
	DO 55 J2=J1,NQ	DGRS1720
	J = (NQ+J1)-J2	DGRS1730
	DO 55 I=1,N	DGRS1740
55	Y(I,J) = Y(I,J)+Y(I,J+1)	DGRS1750
	UP TO 3 CORRECTOR ITERATIONS ARE	DGRS1760
	TAKEN. A CONVERGENCE TEST IS MADE	DGRS1770
	ON THE R.M.S. NORM OF EACH	DGRS1780
	CORRECTION, USING BND, WHICH IS	DGRS1790
	DEPENDENT ON EPS. THE SUM OF THE	DGRS1800
	CORRECTIONS IS ACCUMULATED IN THE	DGRS1810
	VECTOR ERROR(I). THE Y ARRAY IS	DGRS1820
	NOT ALTERED IN THE CORRECTOR LOOP.	DGRS1830
	THE UPDATED Y VECTOR IS STORED	DGRS1840

C	60 DO 65 I=1,N	TEMPORARILY IN SAVE1.	DGRS1850
	65 ERROR(I) = 0.D0		DGRS1860
	M = 0		DGRS1870
	CALL FCN (N,T,Y,SAVE2,eprime,eprime2)		DGRS1880
	NFE = NFE+1		+
	IF (IWEVAL.LE.0) GO TO 95		DGRS1900
C		IF INDICATED, THE MATRIX P = I -	DGRS1910
C		H*EL(1)*J IS REEVALUATED BEFORE	DGRS1920
C		STARTING THE CORRECTOR ITERATION.	DGRS1930
C		IWEVAL IS SET TO 0 AS AN INDICATOR	DGRS1940
C		THAT THIS HAS BEEN DONE. IF MITER	DGRS1950
C		= 1 OR 2, P IS COMPUTED AND	DGRS1960
C		PROCESSED IN PSET. IF MITER = 3,	DGRS1970
C		THE MATRIX USED IS P = I -	DGRS1980
C		H*EL(1)*D, WHERE D IS A DIAGONAL	DGRS1990
C		MATRIX.	DGRS2000
	IWEVAL = 0		DGRS2010
	RC = 1.D0		DGRS2020
	NJE = NJE+1		DGRS2030
	NSTEPJ = NSTEP		DGRS2040
	GO TO (75,70,80), MITER		DGRS2050
70	NFE = NFE+N		DGRS2060
75	CON = -H*EL(1)		DGRS2070
	MITER1 = MITER		DGRS2080
	CALL DGRPS (FCN,FCNJ,Y,N0,CON,MITER1,YMAX,SAVE1,SAVE2,PW,EQUIL,		DGRS2090
	1 IPIV,IER)		DGRS2100
	IF (IER.NE.0) GO TO 155		DGRS2110
	GO TO 125		DGRS2120
80	R = EL(1)*.1D0		DGRS2130
	DO 85 I=1,N		DGRS2140
85	PW(I) = Y(I,1)+R*(H*SAVE2(I)-Y(I,2))		DGRS2150
	CALL FCN (N,T,PW,SAVE1,eprime,eprime2)		DGRS2160
	NFE = NFE+1		+
	HL0 = H*EL(1)		DGRS2180
	DO 90 I=1,N		DGRS2190
	R0 = H*SAVE2(I)-Y(I,2)		DGRS2200
	PW(I) = 1.D0		DGRS2210
	D = .1D0*R0-H*(SAVE1(I)-SAVE2(I))		DGRS2220
	SAVE1(I) = 0.D0		DGRS2230
	IF (DABS(R0).LT.UROUND*YMAX(I)) GO TO 90		DGRS2240
	IF (DABS(D).EQ.0.D0) GO TO 155		DGRS2250
	PW(I) = .1D0*R0/D		DGRS2260
	SAVE1(I) = PW(I)*R0		DGRS2270
90	CONTINUE		DGRS2280
	GO TO 135		DGRS2290
95	IF (MITER.NE.0) GO TO (125,125,105), MITER		DGRS2300
C		IN THE CASE OF FUNCTIONAL ITERATION,	DGRS2310
C		UPDATE Y DIRECTLY FROM THE RESULT	DGRS2320
C		OF THE LAST FCN CALL.	DGRS2330
	D = 0.D0		DGRS2340
	DO 100 I=1,N		DGRS2350
	R = H*SAVE2(I)-Y(I,2)		DGRS2360
	D = D+((R-ERROR(I))/YMAX(I))**2		DGRS2370
	SAVE1(I) = Y(I,1)+EL(1)*R		DGRS2380
100	ERROR(I) = R		DGRS2390
	GO TO 145		DGRS2400
C		IN THE CASE OF THE CHORD METHOD,	DGRS2410
C		COMPUTE THE CORRECTOR ERROR, F SUB	DGRS2420
C		(M), AND SOLVE THE LINEAR SYSTEM	DGRS2430
C		WITH THAT AS RIGHT-HAND SIDE AND P	DGRS2440
			DGRS2450
			DGRS2460

C C C C	<pre> AS COEFFICIENT MATRIX, USING THE LU DECOMPOSITION IF MITER = 1 OR 2. IF MITER = 3, THE COEFFICIENT H*EL(1) IN P IS UPDATED. 105 PHL0 = HLO HLO = H*EL(1) IF (HLO.EQ.PHL0) GO TO 115 R = HLO/PHL0 DO 110 I=1,N D = 1.D0-R*(1.D0-1.D0/PW(I)) IF (DABS(D).EQ.0.D0) GO TO 165 110 PW(I) = 1.D0/D 115 DO 120 I=1,N 120 SAVE1(I) = PW(I)*(H*SAVE2(I) - (Y(I,2)+ERROR(I))) GO TO 135 125 DO 130 I=1,N 130 SAVE1(I) = H*SAVE2(I) - (Y(I,2)+ERROR(I)) IF (NLC.EQ.-1) GO TO 131 NWK = (NLC+NUC+1)*NO+1 CALL LEQT1B(PW,N,NLC,NUC,NO,SAVE1,1,NO,2,PW(NWK),JER) GO TO 135 131 CALL LUELMF(PW,SAVE1,IPIV,N,NO,SAVE1) 135 D = 0.D0 DO 140 I=1,N ERROR(I) = ERROR(I)+SAVE1(I) D = D+(SAVE1(I)/YMAX(I))**2 140 SAVE1(I) = Y(I,1)+EL(1)*ERROR(I) </pre>	<pre> DGRS2470 DGRS2480 DGRS2490 DGRS2500 DGRS251C DGRS2520 DGRS2530 DGRS2540 DGRS2550 DGRS2560 DGRS2570 DGRS2580 DGRS2590 DGRS2600 DGRS2610 DGRS2620 DGRS2630 DGRS2640 DGRS2650 DGRS2660 DGRS2670 DGRS2680 DGRS2690 DGRS2700 DGRS2710 DGRS2720 DGRS2730 DGRS2740 DGRS2750 DGRS2760 DGRS2770 DGRS2780 DGRS2790 DGRS2800 DGRS2810 DGRS2820 + DGRS2840 DGRS2850 DGRS2860 DGRS2870 DGRS2880 DGRS2890 DGRS2900 DGRS2910 DGRS2920 DGRS2930 DGRS2940 DGRS2950 DGRS2960 DGRS2970 DGRS2980 DGRS2990 DGRS3000 DGRS3010 DGRS3020 DGRS3030 DGRS3040 DGRS3050 DGRS3060 DGRS3070 DGRS3080 </pre>
C C C C C C C C C C	<pre> TEST FOR CONVERGENCE. IF M.GT.0, THE SQUARE OF THE CONVERGENCE RATE CONSTANT IS ESTIMATED AS CRATE, AND THIS IS USED IN THE TEST. 145 IF (M.NE.0) CRATE = DMAX1(.9D0*CRATE,D/D1) IF ((D*DMIN1(1.D0,2.D0*CRATE)).LE.BND) GO TO 170 D1 = D M = M+1 IF (M.EQ.3) GO TO 150 CALL FCN(N,T,SAVE1,SAVE2,eprime,eprime2) GO TO 95 </pre>	<pre> DGRS2740 DGRS2750 DGRS2760 DGRS2770 DGRS2780 DGRS2790 DGRS2800 DGRS2810 DGRS2820 + DGRS2840 DGRS2850 DGRS2860 DGRS2870 DGRS2880 DGRS2890 DGRS2900 DGRS2910 DGRS2920 DGRS2930 DGRS2940 DGRS2950 DGRS2960 DGRS2970 DGRS2980 DGRS2990 DGRS3000 DGRS3010 DGRS3020 DGRS3030 DGRS3040 DGRS3050 DGRS3060 DGRS3070 DGRS3080 </pre>
C C C C C C C C C	<pre> THE CORRECTOR ITERATION FAILED TO CONVERGE IN 3 TRIES. IF PARTIALS ARE INVOLVED BUT ARE NOT UP TO DATE, THEY ARE REEVALUATED FOR THE NEXT TRY. OTHERWISE THE Y ARRAY IS RETRACTED TO ITS VALUES BEFORE PREDICTION, AND H IS REDUCED, IF POSSIBLE. IF NOT, A NO-CONVERGENCE EXIT IS TAKEN. 150 NFE = NFE+2 IF (IWEVAL.EQ.-1) GO TO 165 155 T = TOLD RMAX = 2.D0 DO 160 J1=1,NQ DO 160 J2=J1,NQ J = (NQ+J1)-J2 DO 160 I=1,N 160 Y(I,J) = Y(I,J)-Y(I,J+1) IF (DABS(H).LE.HMIN*1.00001D0) GO TO 280 RH = .25D0 IREDO = 1 GO TO 35 165 IWEVAL = MITER GO TO 60 </pre>	<pre> DGRS2740 DGRS2750 DGRS2760 DGRS2770 DGRS2780 DGRS2790 DGRS2800 DGRS2810 DGRS2820 + DGRS2840 DGRS2850 DGRS2860 DGRS2870 DGRS2880 DGRS2890 DGRS2900 DGRS2910 DGRS2920 DGRS2930 DGRS2940 DGRS2950 DGRS2960 DGRS2970 DGRS2980 DGRS2990 DGRS3000 DGRS3010 DGRS3020 DGRS3030 DGRS3040 DGRS3050 DGRS3060 DGRS3070 DGRS3080 </pre>

C
C
C
C
C
C
C

THE CORRECTOR HAS CONVERGED. IWEVAL DGRS3090
IS SET TO -1 IF PARTIAL DGRS3100
DERIVATIVES WERE USED, TO SIGNAL DGRS3110
THAT THEY MAY NEED UPDATING ON DGRS3120
SUBSEQUENT STEPS. THE ERROR TEST DGRS3130
IS MADE AND CONTROL PASSES TO DGRS3140
STATEMENT 190 IF IT FAILS. DGRS3150

```
170 IF (MITER.NE.0) IWEVAL = -1
    NFE = NFE+M
    D = 0.D0
    DO 175 I=1,N
175 D = D+(ERROR(I)/YMAX(I))**2
    IF (D.GT.E) GO TO 190
```

C
C
C
C
C
C
C
C
C
C
C

AFTER A SUCCESSFUL STEP, UPDATE THE DGRS3220
Y ARRAY. CONSIDER CHANGING H IF DGRS3230
IDCOB = 1. OTHERWISE DECREASE DGRS3240
IDCOB BY 1. IF IDCOB IS THEN 1 AND DGRS3250
NQ .LT. MAXDER, THEN ERROR IS DGRS3260
SAVED FOR USE IN A POSSIBLE ORDER DGRS3270
INCREASE ON THE NEXT STEP. IF A DGRS3280
CHANGE IN H IS CONSIDERED, AN DGRS3290
INCREASE OR DECREASE IN ORDER BY DGRS3300
ONE IS CONSIDERED ALSO. A CHANGE DGRS3310
IN H IS MADE ONLY IF IT IS BY A DGRS3320
FACTOR OF AT LEAST 1.1. IF NOT, DGRS3330
IDCOB IS SET TO 10 TO PREVENT DGRS3340
TESTING FOR THAT MANY STEPS. DGRS3350

```
KFLAG = 0
IREDO = 0
NSTEP = NSTEP+1
HUSED = H
NQUSED = NQ
DO 180 J=1,L
DO 180 I=1,N
180 Y(I,J) = Y(I,J)+EL(J)*ERROR(I)
    IF (IDCOB.EQ.1) GO TO 200
    IDCOB = IDCOB-1
    IF (IDCOB.GT.1) GO TO 290
    IF (L.EQ.LMAX) GO TO 290
    DO 185 I=1,N
185 Y(I,LMAX) = ERROR(I)
    GO TO 290
```

C
C
C
C
C
C
C

THE ERROR TEST FAILED. KFLAG KEEPS DGRS3510
TRACK OF MULTIPLE FAILURES. DGRS3520
RESTORE T AND THE Y ARRAY TO THEIR DGRS3530
PREVIOUS VALUES, AND PREPARE TO DGRS3540
TRY THE STEP AGAIN. COMPUTE THE DGRS3550
OPTIMUM STEP SIZE FOR THIS OR ONE DGRS3560
LOWER ORDER. DGRS3570

```
190 KFLAG = KFLAG-1
    T = TOLD
    DO 195 J1=1,NQ
    DO 195 J2=J1,NQ
        J = (NQ+J1)-J2
    DO 195 I=1,N
195 Y(I,J) = Y(I,J)-Y(I,J+1)
    RMAX = 2.D0
    IF (DABS(H).LE.HMIN*1.00001D0) GO TO 270
    IF (KFLAG.LE.-3) GO TO 260
    IREDO = 2
    PR3 = 1.D+20
    GO TO 210
```

DGRS3580
DGRS3590
DGRS3600
DGRS3610
DGRS3620
DGRS3630
DGRS3640
DGRS3650
DGRS3660
DGRS3670
DGRS3680
DGRS3690
DGRS3700

C
C
C
C
C
C
C
C
C
C
C
C
C

REGARDLESS OF THE SUCCESS OR FAILURE DGRS3710
OF THE STEP, FACTORS PR1, PR2, AND DGRS3720
PR3 ARE COMPUTED, BY WHICH H COULD DGRS3730
BE DIVIDED AT ORDER NQ - 1, ORDER DGRS3740
NQ, OR ORDER NQ + 1, RESPECTIVELY. DGRS3750
IN THE CASE OF FAILURE, PR3 = DGRS3760
1.E20 TO AVOID AN ORDER INCREASE. DGRS3770
THE SMALLEST OF THESE IS DGRS3780
DETERMINED AND THE NEW ORDER DGRS3790
CHOSEN ACCORDINGLY. IF THE ORDER DGRS3800
IS TO BE INCREASED, WE COMPUTE ONE DGRS3810
ADDITIONAL SCALED DERIVATIVE. DGRS3820

```

200 PR3 = 1.D+20
    IF (L.EQ.LMAX) GO TO 210
    D1 = 0.D0
    DO 205 I=1,N
205 D1 = D1+((ERROR(I)-Y(I,LMAX))/YMAX(I))**2
    ENQ3 = .5D0/(L+1)
    PR3 = ((D1/EUP)**ENQ3)*1.4D0+1.4D-6
210 ENQ2 = .5D0/L
    PR2 = ((D/E)**ENQ2)*1.2D0+1.2D-6
    PR1 = 1.D+20
    IF (NQ.EQ.1) GO TO 220
    D = 0.D0
    DO 215 I=1,N
215 D = D+(Y(I,L)/YMAX(I))**2
    ENQ1 = .5D0/NQ
    PR1 = ((D/EDN)**ENQ1)*1.3D0+1.3D-6
220 IF (PR2.LE.PR3) GO TO 225
    IF (PR3.LT.PR1) GO TO 235
    GO TO 230
225 IF (PR2.GT.PR1) GO TO 230
    NEWQ = NQ
    RH = 1.D0/PR2
    GO TO 250
230 NEWQ = NQ-1
    RH = 1.D0/PR1
    IF (KFLAG.NE.0.AND.RH.GT.1.D0) RH = 1.D0
    GO TO 250
235 NEWQ = L
    RH = 1.D0/PR3
    IF (RH.LT.1.1D0) GO TO 245
    DO 240 I=1,N
240 Y(I,NEWQ+1) = ERROR(I)*EL(L)/L
    GO TO 255
245 IDOUB = 10
    GO TO 290
250 IF ((KFLAG.EQ.0).AND.(RH.LT.1.1D0)) GO TO 245

```

C
C
C
C
C
C
C

IF THERE IS A CHANGE OF ORDER, RESET DGRS4200
NQ, L, AND THE COEFFICIENTS. IN DGRS4210
ANY CASE H IS RESET ACCORDING TO DGRS4220
RH AND THE Y ARRAY IS RESCALED. DGRS4230
THEN EXIT FROM 285 IF THE STEP WAS DGRS4240
OK, OR REDO THE STEP OTHERWISE. DGRS4250

```

    IF (NEWQ.EQ.NQ) GO TO 35
255 NQ = NEWQ
    L = NQ+1
    IRET = 2
    GO TO 15

```

C
C

CONTROL REACHES THIS SECTION IF 3 OR DGRS4310
MORE FAILURES HAVE OCCURED. IT IS DGRS4320

C
C
C
C
C
C
C
C
C
C

ASSUMED THAT THE DERIVATIVES THAT
HAVE ACCUMULATED IN THE Y ARRAY
HAVE ERRORS OF THE WRONG ORDER.
HENCE THE FIRST DERIVATIVE IS
RECOMPUTED, AND THE ORDER IS SET
TO 1. THEN H IS REDUCED BY A
FACTOR OF 10, AND THE STEP IS
RETRIED. AFTER A TOTAL OF 7
FAILURES, AN EXIT IS TAKEN WITH
KFLAG = -2.

DGRS4330
DGRS4340
DGRS4350
DGRS4360
DGRS4370
DGRS4380
DGRS4390
DGRS4400
DGRS4410
DGRS4420
DGRS4430
DGRS4440
DGRS4450
DGRS4460

```
260 IF (KFLAG.EQ.-7) GO TO 275
    RH = .1D0
    RH = DMAX1(HMIN/DABS(H), RH)
    H = H*RH
    CALL FCN (N,T,Y,SAVE1,eprime,eprime2)
    NFE = NFE+1
    DO 265 I=1,N
265 Y(I,2) = H*SAVE1(I)
    IWEVAL = MITER
    IDOUB = 10
    IF (NQ.EQ.1) GO TO 50
    NQ = 1
    L = 2
    IREF = 3
    GO TO 15
```

+
DGRS4480
DGRS4490
DGRS4500
DGRS4510
DGRS4520
DGRS4530
DGRS4540
DGRS4550
DGRS4560
DGRS4570

C
C
C
C

ALL RETURNS ARE MADE THROUGH THIS
SECTION. H IS SAVED IN HOLD TO
ALLOW THE CALLER TO CHANGE H ON
THE NEXT STEP.

```
270 KFLAG = -1
    GO TO 290
275 KFLAG = -2
    GO TO 290
280 KFLAG = -3
    GO TO 290
285 RMAX = 10.D0
290 HOLD = H
    JSTART = NQ
C--Diagnostic Check of first and second derivatives of E
    if(tcum.eq.told)go to 310
    write(8,300)tcum,step,y(1,1),y(2,1),y(3,1),y(4,1),y(5,1)
300 format(1x,e11.4,1x,15,5(1x,e11.4))
    write(9,305)step,eprime,eprime2
305 format(1x,15,2(1x,e20.13))
    RETURN
    END
```

DGRS4580
DGRS4590
DGRS4600
DGRS4610
DGRS4620
DGRS4630
DGRS4640
DGRS4650
DGRS4660
DGRS4670
DGRS4680
DGRS4690
DGRS4700
+
+
+
+
+
+
DGRS4710
DGRS4720


```

C   IMSL ROUTINE NAME   - DGRCS                               DGRC0010
C                                                                DGRC0020
C-----DGRC0030
C   COMPUTER           - IBM/DOUBLE                           DGRC0040
C                                                                DGRC0050
C   LATEST REVISION    - JANUARY 1, 1978                       DGRC0060
C                                                                DGRC0070
C   PURPOSE            - NUCLEUS CALLED ONLY BY IMSL SUBROUTINE DGEAR DGRC0080
C                                                                DGRC0090
C   PRECISION/HARDWARE - SINGLE AND DOUBLE/H32                 DGRC0100
C                                                                DGRC0110
C                                                                DGRC0120
C                                                                DGRC0130
C   REQD. IMSL ROUTINES - NONE REQUIRED                           DGRC0140
C                                                                DGRC0150
C   NOTATION           - INFORMATION ON SPECIAL NOTATION AND    DGRC0160
C                                                                DGRC0170
C                                                                DGRC0180
C                                                                DGRC0190
C                                                                DGRC0200
C                                                                DGRC0210
C   COPYRIGHT          - 1978 BY IMSL, INC. ALL RIGHTS RESERVED. DGRC0220
C                                                                DGRC0230
C                                                                DGRC0240
C                                                                DGRC0250
C-----DGRC0260
C   SUBROUTINE DGRCS   (METH,NQ,EL,TQ,MAXDER)                   DGRC0270
C                                                                DGRC0280
C                                                                DGRC0290
C                                                                DGRC0300
C                                                                DGRC0310
C                                                                DGRC0320
C                                                                DGRC0330
C                                                                DGRC0340
C                                                                DGRC0350
C                                                                DGRC0360
C                                                                DGRC0370
C                                                                DGRC0380
C                                                                DGRC0390
C                                                                DGRC0400
C                                                                DGRC0410
C                                                                DGRC0420
C                                                                DGRC0430
C                                                                DGRC0440
C                                                                DGRC0450
C                                                                DGRC0460
C                                                                DGRC0470
C                                                                DGRC0480
C                                                                DGRC0490
C                                                                DGRC0500
C                                                                DGRC0510
C                                                                DGRC0520
C                                                                DGRC0530
C                                                                DGRC0540
C                                                                DGRC0550
C                                                                DGRC0560
C                                                                DGRC0570
C                                                                DGRC0580
C                                                                DGRC0590
C                                                                DGRC0600
C                                                                DGRC0610
C                                                                DGRC0620
C
C   SPECIFICATIONS FOR ARGUMENTS
C   INTEGER            METH,NQ,MAXDER
C   REAL               TQ(1)
C   DOUBLE PRECISION  EL(1)
C
C   SPECIFICATIONS FOR LOCAL VARIABLES
C   INTEGER            K
C   REAL              PERTST(12,2,3)
C   DATA
1  PERTST/1.,1.,2.,1.,.3158,.7407E-1,
2  .1391E-1,.2182E-2,.2945E-3,.3492E-4,
3  .3692E-5,.3524E-6,1.,1.,.5,.1667,
4  .4167E-1,7*1.,2.,12.,24.,37.89,
5  53.33,70.08,87.97,106.9,126.7,
6  147.4,168.8,191.0,2.0,4.5,7.333,
7  10.42,13.7,7*1.,12.0,24.0,37.89,
8  53.33,70.08,87.97,106.9,126.7,
9  147.4,168.8,191.0,1.,3.0,6.0,
9  9.167,12.5,8*1./
C
C   FIRST EXECUTABLE STATEMENT
C   GO TO (5,10), METH
5  MAXDER = 12
C   GO TO (15,20,25,30,35,40,45,50,55,60,65,70), NQ
10 MAXDER = 5
C   GO TO (75,80,85,90,95), NQ
C
C   THE FOLLOWING COEFFICIENTS SHOULD BE
C   DEFINED TO MACHINE ACCURACY. FOR A
C   GIVEN ORDER NQ, THEY CAN BE
C   CALCULATED BY USE OF THE
C   GENERATING POLYNOMIAL L(T), WHOSE
C   COEFFICIENTS ARE EL(I) .. L(T) =
C   EL(1) + EL(2)*T + ... +
C   EL(NQ+1)*T**NQ. FOR THE IMPLICIT
C   ADAMS METHODS, L(T) IS GIVEN BY
C   DL/DT = (T+1)*(T+2)* ...
C   *(T+NQ-1)/K, L(-1) = 0, WHERE K =

```

C
C
C
C
C
C
C
C
C
C
C

FACTORIAL(NQ-1). FOR THE GEAR
METHODS, $L(T) = (T+1)*(T+2)* \dots$
 $*(T+NQ)/K$, WHERE $K =$
 $FACTORIAL(NQ)*(1 + 1/2 + \dots +$
 $1/NQ)$. THE ORDER IN WHICH THE
GROUPS APPEAR BELOW IS.. IMPLICIT
ADAMS METHODS OF ORDERS 1 TO 12,
BACKWARD DIFFERENTIATION METHODS
OF ORDERS 1 TO 5.

15 EL(1) = 1.0D0
GO TO 100
20 EL(1) = 0.5D0
EL(3) = 0.5D0
GO TO 100
25 EL(1) = 4.166666666666667D-01
EL(3) = 0.75D0
EL(4) = 1.666666666666667D-01
GO TO 100
30 EL(1) = 0.375D0
EL(3) = 9.166666666666667D-01
EL(4) = 3.333333333333333D-01
EL(5) = 4.166666666666667D-02
GO TO 100
35 EL(1) = 3.486111111111111D-01
EL(3) = 1.041666666666667D0
EL(4) = 4.861111111111111D-01
EL(5) = 1.041666666666667D-01
EL(6) = 8.333333333333333D-03
GO TO 100
40 EL(1) = 3.298611111111111D-01
EL(3) = 1.141666666666667D+00
EL(4) = 0.625D+00
EL(5) = 1.770833333333333D-01
EL(6) = 0.025D+00
EL(7) = 1.388888888888889D-03
GO TO 100
45 EL(1) = 3.155919312169312D-01
EL(3) = 1.225D+00
EL(4) = 7.518518518518519D-01
EL(5) = 2.552083333333333D-01
EL(6) = 4.861111111111111D-02
EL(7) = 4.861111111111111D-03
EL(8) = 1.984126984126984D-04
GO TO 100
50 EL(1) = 3.042245370370370D-01
EL(3) = 1.296428571428571D+00
EL(4) = 8.685185185185185D-01
EL(5) = 3.357638888888889D-01
EL(6) = 7.777777777777778D-02
EL(7) = 1.064814814814815D-02
EL(8) = 7.936507936507937D-04
EL(9) = 2.480158730158730D-05
GO TO 100
55 EL(1) = 2.948680004409171D-01
EL(3) = 1.358928571428571D+00
EL(4) = 9.765542328042328D-01
EL(5) = 4.171875D-01
EL(6) = 1.113541666666667D-01
EL(7) = 0.01875D+00
EL(8) = 1.934523809523810D-03
EL(9) = 1.116071428571429D-04
EL(10) = 2.755731922398589D-06

DGRC0630
DGRC0640
DGRC0650
DGRC0660
DGRC0670
DGRC0680
DGRC0690
DGRC0700
DGRC0710
DGRC0720
DGRC0730
DGRC0740
DGRC0750
DGRC0760
DGRC0770
DGRC0780
DGRC0790
DGRC0800
DGRC0810
DGRC0820
DGRC0830
DGRC0840
DGRC0850
DGRC0860
DGRC0870
DGRC0880
DGRC0890
DGRC0900
DGRC0910
DGRC0920
DGRC0930
DGRC0940
DGRC0950
DGRC0960
DGRC0970
DGRC0980
DGRC0990
DGRC1000
DGRC1010
DGRC1020
DGRC1030
DGRC1040
DGRC1050
DGRC1060
DGRC1070
DGRC1080
DGRC1090
DGRC1100
DGRC1110
DGRC1120
DGRC1130
DGRC1140
DGRC1150
DGRC1160
DGRC1170
DGRC1180
DGRC1190
DGRC1200
DGRC1210
DGRC1220
DGRC1230
DGRC1240

	GO TO 100	DGRC1250
60	EL(1) = 2.869754464285714D-01	DGRC1260
	EL(3) = 1.414484126984127D+00	DGRC1270
	EL(4) = 1.077215608465609D+00	DGRC1280
	EL(5) = 4.985670194003527D-01	DGRC1290
	EL(6) = 1.484375D-01	DGRC1300
	EL(7) = 2.906057098765432D-02	DGRC1310
	EL(8) = 3.720238095238095D-03	DGRC1320
	EL(9) = 2.996858465608466D-04	DGRC1330
	EL(10) = 1.377865961199295D-05	DGRC1340
	EL(11) = 2.755731922398589D-07	DGRC1350
	GO TO 100	DGRC1360
65	EL(1) = 2.801895964439367D-01	DGRC1370
	EL(3) = 1.464484126984127D+00	DGRC1380
	EL(4) = 1.171514550264550D+00	DGRC1390
	EL(5) = 5.793581900352734D-01	DGRC1400
	EL(6) = 1.883228615520282D-01	DGRC1410
	EL(7) = 4.143036265432099D-02	DGRC1420
	EL(8) = 6.211144179894180D-03	DGRC1430
	EL(9) = 6.252066798941799D-04	DGRC1440
	EL(10) = 4.041740152851264D-05	DGRC1450
	EL(11) = 1.515652557319224D-06	DGRC1460
	EL(12) = 2.505210838544172D-08	DGRC1470
	GO TO 100	DGRC1480
70	EL(1) = 2.742655400315991D-01	DGRC1490
	EL(3) = 1.509938672438672D+00	DGRC1500
	EL(4) = 1.260271164021164D+00	DGRC1510
	EL(5) = 6.592341820987654D-01	DGRC1520
	EL(6) = 2.304580026455027D-01	DGRC1530
	EL(7) = 5.569724610523222D-02	DGRC1540
	EL(8) = 9.439484126984127D-03	DGRC1550
	EL(9) = 1.119274966931217D-03	DGRC1560
	EL(10) = 9.093915343915344D-05	DGRC1570
	EL(11) = 4.822530864197531D-06	DGRC1580
	EL(12) = 1.503126503126503D-07	DGRC1590
	EL(13) = 2.087675698786810D-09	DGRC1600
	GO TO 100	DGRC1610
C		DGRC1620
75	EL(1) = 1.0D+00	DGRC1630
	GO TO 100	DGRC1640
80	EL(1) = 6.666666666666667D-01	DGRC1650
	EL(3) = 3.333333333333333D-01	DGRC1660
	GO TO 100	DGRC1670
85	EL(1) = 5.454545454545455D-01	DGRC1680
	EL(3) = EL(1)	DGRC1690
	EL(4) = 9.090909090909091D-02	DGRC1700
	GO TO 100	DGRC1710
90	EL(1) = 0.48D+00	DGRC1720
	EL(3) = 0.7D+00	DGRC1730
	EL(4) = 0.2D+00	DGRC1740
	EL(5) = 0.02D+00	DGRC1750
	GO TO 100	DGRC1760
95	EL(1) = 4.379562043795620D-01	DGRC1770
	EL(3) = 8.211678832116788D-01	DGRC1780
	EL(4) = 3.102189781021898D-01	DGRC1790
	EL(5) = 5.474452554744526D-02	DGRC1800
	EL(6) = 3.649635036496350D-03	DGRC1810
C		DGRC1820
100	DO 105 K=1,3	DGRC1830
	TQ(K) = PERTST(NQ, METH, K)	DGRC1840
105	CONTINUE	DGRC1850
	TQ(4) = .5D0*TQ(2) / (NQ+2)	DGRC1860

RETURN
END

DGRC1870
DGRC1880

```

C   IMSL ROUTINE NAME   - DGRPS                               DGRP0010
C                                                                DGRP0020
C-----DGRP0030
C   COMPUTER           - IBM/DOUBLE                          DGRP0040
C                                                                DGRP0050
C   LATEST REVISION    - NOVEMBER 1, 1984                    DGRP0060
C                                                                DGRP0070
C   PURPOSE            - NUCLEUS CALLED ONLY BY IMSL SUBROUTINE DGEAR DGRP0080
C                                                                DGRP0090
C   PRECISION/HARDWARE - SINGLE AND DOUBLE/H32                DGRP0100
C                                                                DGRP0110
C                                                                - SINGLE/H36,H48,H60    DGRP0120
C                                                                DGRP0130
C   REQD. IMSL ROUTINES - LUDATF,LEQT1B,UERTST,UGETIO         DGRP0140
C                                                                DGRP0150
C   NOTATION           - INFORMATION ON SPECIAL NOTATION AND   DGRP0160
C                                                                CONVENTIONS IS AVAILABLE IN THE MANUAL
C                                                                INTRODUCTION OR THROUGH IMSL ROUTINE UHELP DGRP0170
C                                                                DGRP0180
C   COPYRIGHT          - 1984 BY IMSL, INC. ALL RIGHTS RESERVED. DGRP0190
C                                                                DGRP0200
C                                                                DGRP0210
C   WARRANTY           - IMSL WARRANTS ONLY THAT IMSL TESTING HAS BEEN DGRP0220
C                                                                APPLIED TO THIS CODE. NO OTHER WARRANTY,
C                                                                EXPRESSED OR IMPLIED, IS APPLICABLE.    DGRP0230
C                                                                DGRP0240
C                                                                DGRP0250
C-----DGRP0260
C   SUBROUTINE DGRPS (FCN,FCNJ,Y,NO,CON,MITER,YMAX,SAVE1,SAVE2,PW, DGRP0270
C   *                   EQUIL,IPIV,IER)                       DGRP0280
C                                                                DGRP0290
C                                                                SPECIFICATIONS FOR ARGUMENTS
C   INTEGER             NO,MITER,IPIV(1),IER                  DGRP0300
C   DOUBLE PRECISION    Y(NO,1),CON,YMAX(1),SAVE1(1),SAVE2(1),PW(1), DGRP0310
C   *                   EQUIL(1)                              DGRP0320
C                                                                DGRP0330
C                                                                SPECIFICATIONS FOR LOCAL VARIABLES
C                                                                DGRP0340
C   INTEGER             NC,MFC,KFLAG,JSTART,NQUSED,NSTEP,NFE,NJE,NPW, DGRP0350
C   *                   NSQ,I,J1,J,NERROR,NSAVE1,NSAVE2,NEQUIL,NY,    DGRP0360
C   *                   IDUMMY(23),NLIM,II,IJ,LIM1,LIM2,NB,NLC,NUC,NWK DGRP0370
C   REAL                SDUMMY(4)                             DGRP0380
C   DOUBLE PRECISION    T,H,HMIN,HMAX,EPSC,UROUND,EPSJ,HUSED,D,R0,YJ,R, DGRP0390
C   *                   D1,D2,WA,DUMMY(40)                     DGRP0400
C   COMMON /DBAND/      NLC,NUC                               DGRP0410
C   COMMON /GEAR/       T,H,HMIN,HMAX,EPSC,UROUND,EPSJ,HUSED,DUMMY, DGRP0420
C   *                   SDUMMY,NC,MFC,KFLAG,JSTART,NSQ,NQUSED,NSTEP, DGRP0430
C   *                   NFE,NJE,NPW,NERROR,NSAVE1,NSAVE2,NEQUIL,NY,   DGRP0440
C   *                   IDUMMY                                  DGRP0450
C                                                                DGRP0460
C                                                                DGRP0470
C                                                                DGRP0480
C                                                                DGRP0490
C                                                                DGRP0500
C                                                                DGRP0510
C                                                                DGRP0520
C                                                                DGRP0530
C                                                                DGRP0540
C                                                                DGRP0550
C                                                                DGRP0560
C                                                                DGRP0570
C                                                                DGRP0580
C                                                                DGRP0590
C                                                                DGRP0600
C                                                                DGRP0610
C                                                                DGRP0620

```


	DO 70 J=1,NC	DGRP1250
	YJ = Y(J,1)	DGRP1260
	R = EPSJ*YMAX(J)	DGRP1270
	R = DMAX1(R,R0)	DGRP1280
	Y(J,1) = Y(J,1)+R	DGRP1290
	D = CON/R	DGRP1300
	CALL FCN(NC,T,Y,SAVE1)	DGRP1310
	DO 65 I=1,NC	DGRP1320
65	PW(I+J1) = (SAVE1(I) - SAVE2(I)) * D	DGRP1330
	Y(J,1) = YJ	DGRP1340
	J1 = J1+N0	DGRP1350
	70 CONTINUE	DGRP1360
C	ADD IDENTITY MATRIX.	DGRP1370
	75 J = 1	DGRP1380
	DO 80 I=1,NC	DGRP1390
	PW(J) = PW(J)+1.0D0	DGRP1400
	J = J+(N0+1)	DGRP1410
	80 CONTINUE	DGRP1420
C	DO LU DECOMPOSITION ON P.	DGRP1430
C	CALL LUDATF(PW,PW,NC,N0,0,D1,D2,IPIV,EQUIL,WA,IER)	DGRP1440
	RETURN	DGRP1450
	END	DGRP1460
		DGRP1470

C	IMSL ROUTINE NAME	- DGRIN	DGRI0010
C			DGRI0020
C			DGRI0030
C	COMPUTER	- IBM/DOUBLE	DGRI0040
C			DGRI0050
C	LATEST REVISION	- JANUARY 1, 1978	DGRI0060
C			DGRI0070
C	PURPOSE	- NUCLEUS CALLED ONLY BY IMSL SUBROUTINE DGEAR	DGRI0080
C			DGRI0090
C	PRECISION/HARDWARE	- SINGLE AND DOUBLE/H32	DGRI0100
C		- SINGLE/H36,H48,H60	DGRI0110
C			DGRI0120
C	REQD. IMSL ROUTINES	- NONE REQUIRED	DGRI0130
C			DGRI0140
C	NOTATION	- INFORMATION ON SPECIAL NOTATION AND	DGRI0150
C		CONVENTIONS IS AVAILABLE IN THE MANUAL	DGRI0160
C		INTRODUCTION OR THROUGH IMSL ROUTINE UHELP	DGRI0170
C			DGRI0180
C	COPYRIGHT	- 1978 BY IMSL, INC. ALL RIGHTS RESERVED.	DGRI0190
C			DGRI0200
C	WARRANTY	- IMSL WARRANTS ONLY THAT IMSL TESTING HAS BEEN	DGRI0210
C		APPLIED TO THIS CODE. NO OTHER WARRANTY,	DGRI0220
C		EXPRESSED OR IMPLIED, IS APPLICABLE.	DGRI0230
C			DGRI0240
C			DGRI0250
C			DGRI0260
C	SUBROUTINE DGRIN	(TOUT, Y, NO, Y0)	DGRI0270
C			DGRI0280
C		SPECIFICATIONS FOR ARGUMENTS	DGRI0290
C	INTEGER	NO	DGRI0300
C	DOUBLE PRECISION	TOUT, Y0 (NO), Y (NO, 1)	DGRI0310
C			DGRI0320
C		SPECIFICATIONS FOR LOCAL VARIABLES	DGRI0330
C	INTEGER	NC, MFC, KFLAG, I, L, J, JSTART, NSQ, NQUSED, NSTEP,	DGRI0340
C	1	NFE, NJE, NPW, NERROR, NSAVE1, NSAVE2, NEQUIL, NY,	DGRI0350
C	2	IDUMMY (23)	DGRI0360
C	REAL	SDUMMY (4)	DGRI0370
C	DOUBLE PRECISION	T, H, HMIN, HMAX, EPSC, UROUND, EPSJ, HUSED, S, S1,	DGRI0380
C	1	DUMMY (40)	DGRI0390
C	COMMON /GEAR/	T, H, HMIN, HMAX, EPSC, UROUND, EPSJ, HUSED, DUMMY,	DGRI0400
C	1	SDUMMY, NC, MFC, KFLAG, JSTART, NSQ, NQUSED, NSTEP,	DGRI0410
C	2	NFE, NJE, NPW, NERROR, NSAVE1, NSAVE2, NEQUIL, NY,	DGRI0420
C	3	IDUMMY	DGRI0430
C		FIRST EXECUTABLE STATEMENT	DGRI0440
C	DO 5 I = 1, NC		DGRI0450
C	Y0(I) = Y(I, 1)		DGRI0460
C	5 CONTINUE		DGRI0470
C		THIS SUBROUTINE COMPUTES INTERPOLATED	DGRI0480
C		VALUES OF THE DEPENDENT VARIABLE	DGRI0490
C		Y AND STORES THEM IN Y0. THE	DGRI0500
C		INTERPOLATION IS TO THE	DGRI0510
C		POINT T = TOUT, AND USES THE	DGRI0520
C		NORDSIECK HISTORY ARRAY Y, AS	DGRI0530
C		FOLLOWS..	DGRI0540
C		NO	DGRI0550
C		Y0(I) = SUM Y(I, J+1)*S**J ,	DGRI0560
C		J=0	DGRI0570
C		WHERE S = - (T-TOUT) / H.	DGRI0580
C			DGRI0590
C	L = JSTART + 1		DGRI0600
C	S = (TOUT - T) / H		DGRI0610
C	S1 = 1.0D0		DGRI0620
C	DO 15 J = 2, L		
C	S1 = S1*S		


```
      DO 10 I = 1,NC
      Y0(I) = Y0(I) + S1*Y(I,J)
10    CONTINUE
15    CONTINUE
      RETURN
      END
```

```
DGRI0630
DGRI0640
DGRI0650
DGRI0660
DGRI0670
DGRI0680
```

C	IMSL ROUTINE NAME	- LUDATF	LUDA0010
C			LUDA0020
C			LUDA0030
C	COMPUTER	- IBM/DOUBLE	LUDA0040
C			LUDA0050
C	LATEST REVISION	- JANUARY 1, 1978	LUDA0060
C			LUDA0070
C	PURPOSE	- L-U DECOMPOSITION BY THE CROUT ALGORITHM WITH OPTIONAL ACCURACY TEST.	LUDA0080
C			LUDA0090
C			LUDA0100
C	USAGE	- CALL LUDATF (A, LU, N, IA, IDGT, D1, D2, IPVT, EQUIL, WA, IER)	LUDA0110
C			LUDA0120
C			LUDA0130
C	ARGUMENTS		LUDA0140
C	A	- INPUT MATRIX OF DIMENSION N BY N CONTAINING THE MATRIX TO BE DECOMPOSED.	LUDA0150
C	LU	- REAL OUTPUT MATRIX OF DIMENSION N BY N CONTAINING THE L-U DECOMPOSITION OF A ROWWISE PERMUTATION OF THE INPUT MATRIX. FOR A DESCRIPTION OF THE FORMAT OF LU, SEE EXAMPLE.	LUDA0160
C			LUDA0170
C			LUDA0180
C			LUDA0190
C	N	- INPUT SCALAR CONTAINING THE ORDER OF THE MATRIX A.	LUDA0200
C			LUDA0210
C	IA	- INPUT SCALAR CONTAINING THE ROW DIMENSION OF MATRICES A AND LU EXACTLY AS SPECIFIED IN THE CALLING PROGRAM.	LUDA0220
C			LUDA0230
C	IDGT	- INPUT OPTION. IF IDGT IS GREATER THAN ZERO, THE NON-ZERO ELEMENTS OF A ARE ASSUMED TO BE CORRECT TO IDGT DECIMAL PLACES. LUDATF PERFORMS AN ACCURACY TEST TO DETERMINE IF THE COMPUTED DECOMPOSITION IS THE EXACT DECOMPOSITION OF A MATRIX WHICH DIFFERS FROM THE GIVEN ONE BY LESS THAN ITS UNCERTAINTY. IF IDGT IS EQUAL TO ZERO, THE ACCURACY TEST IS BYPASSED.	LUDA0240
C			LUDA0250
C			LUDA0260
C			LUDA0270
C			LUDA0280
C	D1	- OUTPUT SCALAR CONTAINING ONE OF THE TWO COMPONENTS OF THE DETERMINANT. SEE DESCRIPTION OF PARAMETER D2, BELOW.	LUDA0290
C			LUDA0300
C	D2	- OUTPUT SCALAR CONTAINING ONE OF THE TWO COMPONENTS OF THE DETERMINANT. THE DETERMINANT MAY BE EVALUATED AS (D1) (2**D2).	LUDA0310
C			LUDA0320
C	IPVT	- OUTPUT VECTOR OF LENGTH N CONTAINING THE PERMUTATION INDICES. SEE DOCUMENT (ALGORITHM).	LUDA0330
C			LUDA0340
C	EQUIL	- OUTPUT VECTOR OF LENGTH N CONTAINING RECIPROCAL OF THE ABSOLUTE VALUES OF THE LARGEST (IN ABSOLUTE VALUE) ELEMENT IN EACH ROW.	LUDA0350
C			LUDA0360
C			LUDA0370
C	WA	- ACCURACY TEST PARAMETER, OUTPUT ONLY IF IDGT IS GREATER THAN ZERO. SEE ELEMENT DOCUMENTATION FOR DETAILS.	LUDA0380
C			LUDA0390
C			LUDA0400
C	IER	- ERROR PARAMETER. (OUTPUT) TERMINAL ERROR IER = 129 INDICATES THAT MATRIX A IS ALGORITHMICALLY SINGULAR. (SEE THE CHAPTER L PRELUDE). WARNING ERROR IER = 34 INDICATES THAT THE ACCURACY TEST FAILED. THE COMPUTED SOLUTION MAY BE IN ERROR BY MORE THAN CAN BE ACCOUNTED FOR BY THE UNCERTAINTY OF THE DATA. THIS	LUDA0410
C			LUDA0420
C			LUDA0430
C			LUDA0440
C			LUDA0450
C			LUDA0460
C			LUDA0470
C			LUDA0480
C			LUDA0490
C			LUDA0500
C			LUDA0510
C			LUDA0520
C			LUDA0530
C			LUDA0540
C			LUDA0550
C			LUDA0560
C			LUDA0570
C			LUDA0580
C			LUDA0590
C			LUDA0600
C			LUDA0610
C			LUDA0620

C		WARNING CAN BE PRODUCED ONLY IF IDGT IS	LJDA0630
C		GREATER THAN 0 ON INPUT. SEE CHAPTER L	LJDA0640
C		PRELUDE FOR FURTHER DISCUSSION.	LJDA0650
C			LJDA0660
C	PRECISION/HARDWARE	- SINGLE AND DOUBLE/H32	LJDA0670
C		- SINGLE/H36,H48,H60	LJDA0680
C			LJDA0690
C	REQD. IMSL ROUTINES	- UERTST,UGETIO	LJDA0700
C			LJDA0710
C	NOTATION	- INFORMATION ON SPECIAL NOTATION AND	LJDA0720
C		CONVENTIONS IS AVAILABLE IN THE MANUAL	LJDA0730
C		INTRODUCTION OR THROUGH IMSL ROUTINE UHELP	LJDA0740
C			LJDA0750
C	REMARKS	A TEST FOR SINGULARITY IS MADE AT TWO LEVELS:	LJDA0760
C		1. A ROW OF THE ORIGINAL MATRIX A IS NULL.	LJDA0770
C		2. A COLUMN BECOMES NULL IN THE FACTORIZATION PROCESS.	LJDA0780
C			LJDA0790
C	COPYRIGHT	- 1978 BY IMSL, INC. ALL RIGHTS RESERVED.	LJDA0800
C			LJDA0810
C	WARRANTY	- IMSL WARRANTS ONLY THAT IMSL TESTING HAS BEEN	LJDA0820
C		APPLIED TO THIS CODE. NO OTHER WARRANTY,	LJDA0830
C		EXPRESSED OR IMPLIED, IS APPLICABLE.	LJDA0840
C			LJDA0850
C			LJDA0860
C			LJDA0870
C		SUBROUTINE LUDATF (A, LU, N, IA, IDGT, D1, D2, IPVT, EQUIL, WA, IER)	LJDA0880
C			LJDA0890
C	DIMENSION	A(IA,1), LU(IA,1), IPVT(1), EQUIL(1)	LJDA0900
C	DOUBLE PRECISION	A, LU, D1, D2, EQUIL, WA, ZERO, ONE, FOUR, SIXTN, SIXTH,	LJDA0910
C	*	RN, WREL, BIGA, BIG, P, SUM, AI, WI, T, TEST, Q	LJDA0920
C	DATA	ZERO, ONE, FOUR, SIXTN, SIXTH/0.DO, 1.DO, 4.DO,	LJDA0930
C	*	16.DO, .0625D0/	LJDA0940
C		FIRST EXECUTABLE STATEMENT	LJDA0950
C		INITIALIZATION	LJDA0960
C		IER = 0	LJDA0970
C		RN = N	LJDA0980
C		WREL = ZERO	LJDA0990
C		D1 = ONE	LJDA1000
C		D2 = ZERO	LJDA1010
C		BIGA = ZERO	LJDA1020
C		DO 10 I=1,N	LJDA1030
C		BIG = ZERO	LJDA1040
C		DO 5 J=1,N	LJDA1050
C		P = A(I,J)	LJDA1060
C		LU(I,J) = P	LJDA1070
C		P = DABS(P)	LJDA1080
C		IF (P .GT. BIG) BIG = P	LJDA1090
C	5	CONTINUE	LJDA1100
C		IF (BIG .GT. BIGA) BIGA = BIG	LJDA1110
C		IF (BIG .EQ. ZERO) GO TO 110	LJDA1120
C		EQUIL(I) = ONE/BIG	LJDA1130
C	10	CONTINUE	LJDA1140
C		DO 105 J=1,N	LJDA1150
C		JM1 = J-1	LJDA1160
C		IF (JM1 .LT. 1) GO TO 40	LJDA1170
C		COMPUTE U(I,J), I=1,...,J-1	LJDA1180
C		DO 35 I=1,JM1	LJDA1190
C		SUM = LU(I,J)	LJDA1200
C		IM1 = I-1	LJDA1210
C		IF (IDGT .EQ. 0) GO TO 25	LJDA1220
C		WITH ACCURACY TEST	LJDA1230
C		AI = DABS(SUM)	LJDA1240

	WI = ZERO	LUDA1250
	IF (IM1 .LT. 1) GO TO 20	LUDA1260
	DO 15 K=1, IM1	LUDA1270
	T = LU(I,K)*LU(K,J)	LUDA1280
	SUM = SUM-T	LUDA1290
	WI = WI+DABS(T)	LUDA1300
15	CONTINUE	LUDA1310
	LU(I,J) = SUM	LUDA1320
20	WI = WI+DABS(SUM)	LUDA1330
	IF (AI .EQ. ZERO) AI = BIGA	LUDA1340
	TEST = WI/AI	LUDA1350
	IF (TEST .GT. WREL) WREL = TEST	LUDA1360
	GO TO 35	LUDA1370
C		WITHOUT ACCURACY
25	IF (IM1 .LT. 1) GO TO 35	LUDA1380
	DO 30 K=1, IM1	LUDA1390
	SUM = SUM-LU(I,K)*LU(K,J)	LUDA1400
30	CONTINUE	LUDA1410
	LU(I,J) = SUM	LUDA1420
35	CONTINUE	LUDA1430
40	P = ZERO	LUDA1440
C		COMPUTE U(J,J) AND L(I,J), I=J+1, ...,
	DO 70 I=J,N	LUDA1460
	SUM = LU(I,J)	LUDA1470
	IF (IDGT .EQ. 0) GO TO 55	LUDA1480
C		WITH ACCURACY TEST
	AI = DABS(SUM)	LUDA1490
	WI = ZERO	LUDA1500
	IF (JM1 .LT. 1) GO TO 50	LUDA1510
	DO 45 K=1, JM1	LUDA1520
	T = LU(I,K)*LU(K,J)	LUDA1530
	SUM = SUM-T	LUDA1540
	WI = WI+DABS(T)	LUDA1550
45	CONTINUE	LUDA1560
	LU(I,J) = SUM	LUDA1570
50	WI = WI+DABS(SUM)	LUDA1580
	IF (AI .EQ. ZERO) AI = BIGA	LUDA1590
	TEST = WI/AI	LUDA1600
	IF (TEST .GT. WREL) WREL = TEST	LUDA1610
	GO TO 65	LUDA1620
C		WITHOUT ACCURACY TEST
55	IF (JM1 .LT. 1) GO TO 65	LUDA1630
	DO 60 K=1, JM1	LUDA1640
	SUM = SUM-LU(I,K)*LU(K,J)	LUDA1650
60	CONTINUE	LUDA1660
	LU(I,J) = SUM	LUDA1670
65	Q = EQUIL(I)*DABS(SUM)	LUDA1680
	IF (P .GE. Q) GO TO 70	LUDA1690
	P = Q	LUDA1700
	IMAX = I	LUDA1710
70	CONTINUE	LUDA1720
C		TEST FOR ALGORITHMIC SINGULARITY
	IF (RN+P .EQ. RN) GO TO 110	LUDA1730
	IF (J .EQ. IMAX) GO TO 80	LUDA1740
C		INTERCHANGE ROWS J AND IMAX
	D1 = -D1	LUDA1750
	DO 75 K=1, N	LUDA1760
	P = LU(IMAX, K)	LUDA1770
	LU(IMAX, K) = LU(J, K)	LUDA1780
	LU(J, K) = P	LUDA1790
75	CONTINUE	LUDA1800
	EQUIL(IMAX) = EQUIL(J)	LUDA1810
		LUDA1820
		LUDA1830
		LUDA1840
		LUDA1850
		LUDA1860

80	IPVT(J) = IMAX	LUDA1870
	D1 = D1*LU(J,J)	LUDA1880
85	IF (DABS(D1) .LE. ONE) GO TO 90	LUDA1890
	D1 = D1*SIXTH	LUDA1900
	D2 = D2+FOUR	LUDA1910
	GO TO 85	LUDA1920
90	IF (DABS(D1) .GE. SIXTH) GO TO 95	LUDA1930
	D1 = D1*SIXTH	LUDA1940
	D2 = D2-FOUR	LUDA1950
	GO TO 90	LUDA1960
95	CONTINUE	LUDA1970
	JP1 = J+1	LUDA1980
	IF (JP1 .GT. N) GO TO 105	LUDA1990
C		LUDA2000
		LUDA2010
		LUDA2020
		LUDA2030
100	CONTINUE	LUDA2040
105	CONTINUE	LUDA2050
C		LUDA2060
		LUDA2070
		LUDA2080
		LUDA2090
		LUDA2100
		LUDA2110
		LUDA2120
C		LUDA2130
		LUDA2140
110	IER = 129	LUDA2150
	D1 = ZERO	LUDA2160
	D2 = ZERO	LUDA2170
9000	CONTINUE	LUDA2180
C		LUDA2190
		LUDA2200
9005	RETURN	LUDA2210
	END	

C	IMSL ROUTINE NAME	- LUELMF	LUJEF0010
C			LUJEF0020
C			LUJEF0030
C	COMPUTER	- IBM/DOUBLE	LUJEF0040
C			LUJEF0050
C	LATEST REVISION	- JANUARY 1, 1978	LUJEF0060
C			LUJEF0070
C	PURPOSE	- ELIMINATION PART OF SOLUTION OF AX=B (FULL STORAGE MODE)	LUJEF0080
C			LUJEF0090
C			LUJEF0100
C	USAGE	- CALL LUJELMF (A,B,IPVT,N,IA,X)	LUJEF0110
C			LUJEF0120
C			LUJEF0130
C	ARGUMENTS	A	- A = LU (THE RESULT COMPUTED IN THE IMSL ROUTINE LUJATF) WHERE L IS A LOWER TRIANGULAR MATRIX WITH ONES ON THE MAIN DIAGONAL. U IS UPPER TRIANGULAR. L AND U ARE STORED AS A SINGLE MATRIX A AND THE UNIT DIAGONAL OF L IS NOT STORED. (INPUT)
C			LUJEF0140
C			LUJEF0150
C			LUJEF0160
C			LUJEF0170
C			LUJEF0180
C			LUJEF0190
C		B	- B IS A VECTOR OF LENGTH N ON THE RIGHT HAND SIDE OF THE EQUATION AX=B. (INPUT)
C			LUJEF0200
C		IPVT	- THE PERMUTATION MATRIX RETURNED FROM THE IMSL ROUTINE LUJATF, STORED AS AN N LENGTH VECTOR. (INPUT)
C			LUJEF0210
C			LUJEF0220
C			LUJEF0230
C			LUJEF0240
C		N	- ORDER OF A AND NUMBER OF ROWS IN B. (INPUT)
C			LUJEF0250
C		IA	- ROW DIMENSION OF A EXACTLY AS SPECIFIED IN THE DIMENSION STATEMENT IN THE CALLING PROGRAM. (INPUT)
C			LUJEF0260
C			LUJEF0270
C		X	- THE RESULT X. (OUTPUT)
C			LUJEF0280
C			LUJEF0290
C			LUJEF0300
C	PRECISION/HARDWARE	- SINGLE AND DOUBLE/H32	LUJEF0310
C		- SINGLE/H36,H48,H60	LUJEF0320
C			LUJEF0330
C	REQD. IMSL ROUTINES	- NONE REQUIRED	LUJEF0340
C			LUJEF0350
C	NOTATION	- INFORMATION ON SPECIAL NOTATION AND CONVENTIONS IS AVAILABLE IN THE MANUAL INTRODUCTION OR THROUGH IMSL ROUTINE UHELP	LUJEF0360
C			LUJEF0370
C			LUJEF0380
C			LUJEF0390
C	COPYRIGHT	- 1978 BY IMSL, INC. ALL RIGHTS RESERVED.	LUJEF0400
C			LUJEF0410
C	WARRANTY	- IMSL WARRANTS ONLY THAT IMSL TESTING HAS BEEN APPLIED TO THIS CODE. NO OTHER WARRANTY, EXPRESSED OR IMPLIED, IS APPLICABLE.	LUJEF0420
C			LUJEF0430
C			LUJEF0440
C			LUJEF0450
C			LUJEF0460
C			LUJEF0470
C	SUBROUTINE LUJELMF (A,B,IPVT,N,IA,X)		LUJEF0480
C			LUJEF0490
C	DIMENSION	A(IA,1),B(1),IPVT(1),X(1)	LUJEF0500
C	DOUBLE PRECISION	A,B,X,SUM	LUJEF0510
C		FIRST EXECUTABLE STATEMENT	LUJEF0520
C		SOLVE LY = B FOR Y	LUJEF0530
C	DO 5 I=1,N		LUJEF0540
C	5 X(I) = B(I)		LUJEF0550
C	IW = 0		LUJEF0560
C	DO 20 I=1,N		LUJEF0570
C	IP = IPVT(I)		LUJEF0580
C	SUM = X(IP)		LUJEF0590
C	X(IP) = X(I)		LUJEF0600
C	IF (IW .EQ. 0) GO TO 15		LUJEF0610
C	IM1 = I-1		LUJEF0620

```

DO 10 J=IW,IM1
    SUM = SUM-A(I,J)*X(J)
10  CONTINUE
    GO TO 20
15  IF (SUM .NE. 0.D0) IW = I
20  X(I) = SUM
C
DO 30 IB=1,N
    I = N+1-IB
    IP1 = I+1
    SUM = X(I)
    IF (IP1 .GT. N) GO TO 30
    DO 25 J=IP1,N
        SUM = SUM-A(I,J)*X(J)
25  CONTINUE
30  X(I) = SUM/A(I,I)
    RETURN
    END

```

SOLVE UX = Y FOR X

```

LJEF0630
LJEF0640
LJEF0650
LJEF0660
LJEF0670
LJEF0680
LJEF0690
LJEF0700
LJEF0710
LJEF0720
LJEF0730
LJEF0740
LJEF0750
LJEF0760
LJEF0770
LJEF0780
LJEF0790
LJEF0800

```

C	IMSL ROUTINE NAME	- LEQT1B	LE1B0010
C			LE1B0020
C	-----		LE1B0030
C	COMPUTER	- IBM/DOUBLE	LE1B0040
C			LE1B0050
C	LATEST REVISION	- JANUARY 1, 1978	LE1B0060
C			LE1B0070
C	PURPOSE	- LINEAR EQUATION SOLUTION - BAND STORAGE MODE - SPACE ECONOMIZER SOLUTION	LE1B0080
C			LE1B0090
C			LE1B0100
C	USAGE	- CALL LEQT1B (A,N,NLC,NUC,IA,B,M,IB,IJOB,XL, IER)	LE1B0110
C			LE1B0120
C			LE1B0130
C	ARGUMENTS	A	LE1B0140
C		- INPUT/OUTPUT MATRIX OF DIMENSION N BY (NUC+NLC+1). SEE PARAMETER IJOB.	LE1B0150
C		N	LE1B0160
C		- ORDER OF MATRIX A AND THE NUMBER OF ROWS IN B. (INPUT)	LE1B0170
C		NLC	LE1B0180
C		- NUMBER OF LOWER CODIAGONALS IN MATRIX A. (INPUT)	LE1B0190
C		NUC	LE1B0200
C		- NUMBER OF UPPER CODIAGONALS IN MATRIX A. (INPUT)	LE1B0210
C		IA	LE1B0220
C		- ROW DIMENSION OF MATRIX A EXACTLY AS SPECIFIED IN THE DIMENSION STATEMENT IN THE CALLING PROGRAM. (INPUT)	LE1B0230
C			LE1B0240
C		B	LE1B0250
C		- INPUT/OUTPUT MATRIX OF DIMENSION N BY M. ON INPUT, B CONTAINS THE M RIGHT-HAND SIDES OF THE EQUATION AX = B. ON OUTPUT, THE SOLUTION MATRIX X REPLACES B. IF IJOB = 1, B IS NOT USED.	LE1B0260
C			LE1B0270
C			LE1B0280
C		M	LE1B0290
C		- NUMBER OF RIGHT HAND SIDES (COLUMNS IN B). (INPUT)	LE1B0300
C			LE1B0310
C		IB	LE1B0320
C		- ROW DIMENSION OF MATRIX B EXACTLY AS SPECIFIED IN THE DIMENSION STATEMENT IN THE CALLING PROGRAM. (INPUT)	LE1B0330
C			LE1B0340
C		IJOB	LE1B0350
C		- INPUT OPTION PARAMETER. IJOB = I IMPLIES WHEN I = 0, FACTOR THE MATRIX A AND SOLVE THE EQUATION AX = B. ON INPUT, A CONTAINS THE COEFFICIENT MATRIX OF THE EQUATION AX = B, WHERE A IS ASSUMED TO BE AN N BY N BAND MATRIX. A IS STORED IN BAND STORAGE MODE AND THEREFORE HAS DIMENSION N BY (NLC+NUC+1). ON OUTPUT, A IS REPLACED BY THE U MATRIX OF THE L-U DECOMPOSITION OF A ROWWISE PERMUTATION OF MATRIX A. U IS STORED IN BAND STORAGE MODE.	LE1B0360
C			LE1B0370
C			LE1B0380
C			LE1B0390
C			LE1B0400
C			LE1B0410
C			LE1B0420
C			LE1B0430
C			LE1B0440
C			LE1B0450
C			LE1B0460
C		I = 1, FACTOR THE MATRIX A. A CONTAINS THE SAME INPUT/OUTPUT INFORMATION AS IF IJOB = 0.	LE1B0470
C			LE1B0480
C			LE1B0490
C		I = 2, SOLVE THE EQUATION AX = B. THIS OPTION IMPLIES THAT LEQT1B HAS ALREADY BEEN CALLED USING IJOB = 0 OR 1 SO THAT THE MATRIX A HAS ALREADY BEEN FACTORED. IN THIS CASE, OUTPUT MATRICES A AND XL MUST HAVE BEEN SAVED FOR REUSE IN THE CALL TO LEQT1B.	LE1B0500
C			LE1B0510
C			LE1B0520
C			LE1B0530
C			LE1B0540
C			LE1B0550
C			LE1B0560
C		XL	LE1B0570
C		- WORK AREA OF DIMENSION N*(NLC+1). THE FIRST NLC*N LOCATIONS OF XL CONTAIN COMPONENTS OF THE L MATRIX OF THE L-U DECOMPOSITION OF A ROWWISE PERMUTATION OF A. THE LAST N LOCATIONS CONTAIN THE PIVOT INDICES.	LE1B0580
C			LE1B0590
C			LE1B0600
C			LE1B0610
C		IER	LE1B0620
C		- ERROR PARAMETER. (OUTPUT)	

DO 40 I = JBEG,N	LE1B1250
P = ZERO	LE1B1260
DO 30 J = 1,NN	LE1B1270
Q = DABS(A(I,J))	LE1B1280
IF (Q .GT. P) P = Q	LE1B1290
30 CONTINUE	LE1B1300
IF (P .EQ. ZERO) GO TO 135	LE1B1310
XL(I,NLC1) = ONE/P	LE1B1320
IF (I .EQ. JEND) GO TO 37	LE1B1330
IF (I .LT. JEND) GO TO 40	LE1B1340
K = NN+1	LE1B1350
DO 35 J = K,NC	LE1B1360
A(I,J) = ZERO	LE1B1370
35 CONTINUE	LE1B1380
37 NN = NN-1	LE1B1390
40 CONTINUE	LE1B1400
L = NLC	LE1B1410
C	LE1B1420
	LE1B1430
	LE1B1440
	LE1B1450
	LE1B1460
	LE1B1470
	LE1B1480
	LE1B1490
	LE1B1500
	LE1B1510
	LE1B1520
	LE1B1530
	LE1B1540
	LE1B1550
	LE1B1560
	LE1B1570
	LE1B1580
	LE1B1590
	LE1B1600
	LE1B1610
	LE1B1620
	LE1B1630
	LE1B1640
	LE1B1650
	LE1B1660
	LE1B1670
	LE1B1680
	LE1B1690
	LE1B1700
	LE1B1710
	LE1B1720
	LE1B1730
	LE1B1740
	LE1B1750
	LE1B1760
	LE1B1770
	LE1B1780
	LE1B1790
	LE1B1800
	LE1B1810
	LE1B1820
	LE1B1830
	LE1B1840
	LE1B1850
	LE1B1860

	L-U DECOMPOSITION
DO 75 K = 1,N	
P = DABS(A(K,1))*XL(K,NLC1)	
I = K	
IF (L .LT. N) L = L+1	
K1 = K+1	
IF (K1 .GT. L) GO TO 50	
DO 45 J = K1,L	
Q = DABS(A(J,1))*XL(J,NLC1)	
IF (Q .LE. P) GO TO 45	
P = Q	
I = J	
45 CONTINUE	
50 XL(I,NLC1) = XL(K,NLC1)	
XL(K,NLC1) = I	
C	SINGULARITY FOUND
Q = RN+P	
IF (Q .EQ. RN) GO TO 135	
C	INTERCHANGE ROWS I AND K
IF (K .EQ. I) GO TO 60	
DO 55 J = 1,NC	
P = A(K,J)	
A(K,J) = A(I,J)	
A(I,J) = P	
55 CONTINUE	
60 IF (K1 .GT. L) GO TO 75	
DO 70 I = K1,L	
P = A(I,1)/A(K,1)	
IK = I-K	
XL(K1,IK) = P	
DO 65 J = 2,NC	
A(I,J-1) = A(I,J) - P*A(K,J)	
65 CONTINUE	
A(I,NC) = ZERO	
70 CONTINUE	
75 CONTINUE	
IF (IJOB .EQ. 1) GO TO 9005	
C	FORWARD SUBSTITUTION
80 L = NLC	
DO 105 K = 1,N	
I = XL(K,NLC1)	
IF (I .EQ. K) GO TO 90	
DO 85 J = 1,M	
P = B(K,J)	
B(K,J) = B(I,J)	

	B(I,J) = P	LE1B1870
85	CONTINUE	LE1B1880
90	IF (L .LT. N) L = L+1	LE1B1890
	K1 = K+1	LE1B1900
	IF (K1 .GT. L) GO TO 105	LE1B1910
	DO 100 I = K1,L	LE1B1920
	IK = I-K	LE1B1930
	P = XL(K1,IK)	LE1B1940
	DO 95 J = 1,M	LE1B1950
	B(I,J) = B(I,J) - P*B(K,J)	LE1B1960
95	CONTINUE	LE1B1970
100	CONTINUE	LE1B1980
105	CONTINUE	LE1B1990
C		LE1B2000
	BACKWARD SUBSTITUTION	LE1B2010
	JBEG = NUC+NLC	LE1B2020
	DO 125 J = 1,M	LE1B2030
	L = 1	LE1B2040
	K1 = N+1	LE1B2050
	DO 120 I = 1,N	LE1B2060
	K = K1-I	LE1B2070
	P = B(K,J)	LE1B2080
	IF (L .EQ. 1) GO TO 115	LE1B2090
	DO 110 KK = 2,L	LE1B2100
	IK = KK+K	LE1B2110
	P = P - A(K, KK) * B(IK-1, J)	LE1B2120
110	CONTINUE	LE1B2130
115	B(K,J) = P/A(K,1)	LE1B2140
	IF (L .LE. JBEG) L = L+1	LE1B2150
120	CONTINUE	LE1B2160
125	CONTINUE	LE1B2170
	GO TO 9005	LE1B2180
135	IER = 129	LE1B2190
9000	CONTINUE	LE1B2200
	CALL UERTST(IER, 6HLEQT1B)	LE1B2210
9005	RETURN	LE1B2220
	END	

```

C   IMSL ROUTINE NAME   - UERTST                               UERT0010
C                                                                UERT0020
C-----UERT0030
C   COMPUTER           - IBM/SINGLE                            UERT0040
C                                                                UERT0050
C   LATEST REVISION    - JUNE 1, 1982                        UERT0060
C                                                                UERT0070
C   PURPOSE            - PRINT A MESSAGE REFLECTING AN ERROR CONDITION UERT0080
C                                                                UERT0090
C   USAGE              - CALL UERTST (IER,NAME)              UERT0100
C                                                                UERT0110
C   ARGUMENTS          IER  - ERROR PARAMETER. (INPUT)       UERT0120
C                                                                UERT0130
C                       IER = I+J WHERE                       UERT0140
C                       I = 128 IMPLIES TERMINAL ERROR MESSAGE, UERT0150
C                       I = 64 IMPLIES WARNING WITH FIX MESSAGE, UERT0160
C                       I = 32 IMPLIES WARNING MESSAGE.       UERT0170
C                       J = ERROR CODE RELEVANT TO CALLING    UERT0180
C                       ROUTINE.                               UERT0190
C                       NAME - A CHARACTER STRING OF LENGTH SIX PROVIDING UERT0200
C                             THE NAME OF THE CALLING ROUTINE. (INPUT) UERT0210
C                                                                UERT0220
C   PRECISION/HARDWARE - SINGLE/ALL                          UERT0230
C                                                                UERT0240
C   REQD. IMSL ROUTINES - UGETIO,USPKD                       UERT0250
C                                                                UERT0260
C   NOTATION           - INFORMATION ON SPECIAL NOTATION AND  UERT0270
C                       CONVENTIONS IS AVAILABLE IN THE MANUAL UERT0280
C                       INTRODUCTION OR THROUGH IMSL ROUTINE UHELP UERT0290
C                                                                UERT0300
C   REMARKS            THE ERROR MESSAGE PRODUCED BY UERTST IS WRITTEN UERT0310
C                       TO THE STANDARD OUTPUT UNIT. THE OUTPUT UNIT UERT0320
C                       NUMBER CAN BE DETERMINED BY CALLING UGETIO AS UERT0330
C                       FOLLOWS.. CALL UGETIO(1,NIN,NOUT).     UERT0340
C                       THE OUTPUT UNIT NUMBER CAN BE CHANGED BY CALLING UERT0350
C                       UGETIO AS FOLLOWS..                    UERT0360
C                       NIN = 0                                  UERT0370
C                       NOUT = NEW OUTPUT UNIT NUMBER          UERT0380
C                       CALL UGETIO(3,NIN,NOUT)                UERT0390
C                       SEE THE UGETIO DOCUMENT FOR MORE DETAILS. UERT0400
C                                                                UERT0410
C   COPYRIGHT          - 1982 BY IMSL, INC. ALL RIGHTS RESERVED. UERT0420
C                                                                UERT0430
C   WARRANTY           - IMSL WARRANTS ONLY THAT IMSL TESTING HAS BEEN UERT0440
C                       APPLIED TO THIS CODE. NO OTHER WARRANTY, UERT0450
C                       EXPRESSED OR IMPLIED, IS APPLICABLE.  UERT0460
C                                                                UERT0470
C-----UERT0480
C   SUBROUTINE UERTST (IER,NAME)                               UERT0490
C                                                                UERT0500
C                       SPECIFICATIONS FOR ARGUMENTS           UERT0510
C   INTEGER            IER                                     UERT0520
C   INTEGER            NAME(1)                                UERT0530
C                                                                UERT0540
C                       SPECIFICATIONS FOR LOCAL VARIABLES     UERT0550
C   INTEGER            I, IEQ, IEQDF, IOUNIT, LEVEL, LEVOLD, NAMEQ(6), UERT0560
C   *                  NAMSET(6), NAMUPK(6), NIN, NMTB        UERT0570
C   DATA              NAMSET/1HU, 1HE, 1HR, 1HS, 1HE, 1HT/   UERT0580
C   DATA              NAMEQ/6*1H /                            UERT0590
C   DATA              LEVEL/4/, IEQDF/0/, IEQ/1H=/           UERT0600
C                                                                UERT0610
C                       UNPACK NAME INTO NAMUPK                UERT0620
C                                                                UERT0630
C                       FIRST EXECUTABLE STATEMENT             UERT0640
C   CALL USPKD (NAME,6,NAMUPK,NMTB)                            UERT0650

```

C		GET OUTPUT UNIT NUMBER	UERT0630
	CALL	UGETIO(1,NIN,IOUNIT)	UERT0640
C		CHECK IER	UERT0650
	IF	(IER.GT.999) GO TO 25	UERT0660
	IF	(IER.LT.-32) GO TO 55	UERT0670
	IF	(IER.LE.128) GO TO 5	UERT0680
	IF	(LEVEL.LT.1) GO TO 30	UERT0690
C		PRINT TERMINAL MESSAGE	UERT0700
	IF	(IEQDF.EQ.1) WRITE (IOUNIT,35) IER,NAMEQ,IEQ,NAMUPK	UERT0710
	IF	(IEQDF.EQ.0) WRITE (IOUNIT,35) IER,NAMUPK	UERT0720
		GO TO 30	UERT0730
	5	IF (IER.LE.64) GO TO 10	UERT0740
		IF (LEVEL.LT.2) GO TO 30	UERT0750
C		PRINT WARNING WITH FIX MESSAGE	UERT0760
	IF	(IEQDF.EQ.1) WRITE (IOUNIT,40) IER,NAMEQ,IEQ,NAMUPK	UERT0770
	IF	(IEQDF.EQ.0) WRITE (IOUNIT,40) IER,NAMUPK	UERT0780
		GO TO 30	UERT0790
	10	IF (IER.LE.32) GO TO 15	UERT0800
C		PRINT WARNING MESSAGE	UERT0810
	IF	(LEVEL.LT.3) GO TO 30	UERT0820
	IF	(IEQDF.EQ.1) WRITE (IOUNIT,45) IER,NAMEQ,IEQ,NAMUPK	UERT0830
	IF	(IEQDF.EQ.0) WRITE (IOUNIT,45) IER,NAMUPK	UERT0840
		GO TO 30	UERT0850
	15	CONTINUE	UERT0860
C		CHECK FOR UERSET CALL	UERT0870
	DO	20 I=1,6	UERT0880
		IF (NAMUPK(I).NE.NAMSET(I)) GO TO 25	UERT0890
	20	CONTINUE	UERT0900
		LEVOLD = LEVEL	UERT0910
		LEVEL = IER	UERT0920
		IER = LEVOLD	UERT0930
		IF (LEVEL.LT.0) LEVEL = 4	UERT0940
		IF (LEVEL.GT.4) LEVEL = 4	UERT0950
		GO TO 30	UERT0960
	25	CONTINUE	UERT0970
		IF (LEVEL.LT.4) GO TO 30	UERT0980
C		PRINT NON-DEFINED MESSAGE	UERT0990
	IF	(IEQDF.EQ.1) WRITE (IOUNIT,50) IER,NAMEQ,IEQ,NAMUPK	UERT1000
	IF	(IEQDF.EQ.0) WRITE (IOUNIT,50) IER,NAMUPK	UERT1010
	30	IEQDF = 0	UERT1020
		RETURN	UERT1030
	35	FORMAT(19H *** TERMINAL ERROR,10X,7H(IER = ,I3,	UERT1040
	1	20H) FROM IMSL ROUTINE ,6A1,A1,6A1)	UERT1050
	40	FORMAT(27H *** WARNING WITH FIX ERROR,2X,7H(IER = ,I3,	UERT1060
	1	20H) FROM IMSL ROUTINE ,6A1,A1,6A1)	UERT1070
	45	FORMAT(18H *** WARKING ERROR,11X,7H(IER = ,I3,	UERT1080
	1	20H) FROM IMSL ROUTINE ,6A1,A1,6A1)	UERT1090
	50	FORMAT(20H *** UNDEFINED ERROR,9X,7H(IER = ,I5,	UERT1100
	1	20H) FROM IMSL ROUTINE ,6A1,A1,6A1)	UERT1110
C		SAVE P FOR P = R CASE	UERT1120
C		P IS THE PAGE NAMUPK	UERT1130
C		R IS THE ROUTINE NAMUPK	UERT1140
C			UERT1150
	55	IEQDF = 1	UERT1160
		DO 60 I=1,6	UERT1170
	60	NAMEQ(I) = NAMUPK(I)	UERT1180
	65	RETURN	UERT1190
		END	UERT1200

C	IMSL ROUTINE NAME	- UGETIO	UGET0010
C			UGET0020
C	-----	-----	UGET0030
C	COMPUTER	- IBM/SINGLE	UGET0040
C			UGET0050
C	LATEST REVISION	- JUNE 1, 1981	UGET0060
C			UGET0070
C	PURPOSE	- TO RETRIEVE CURRENT VALUES AND TO SET NEW VALUES FOR INPUT AND OUTPUT UNIT IDENTIFIERS.	UGET0080
C			UGET0090
C	USAGE	- CALL UGETIO (IOPT, NIN, NOUT)	UGET0100
C			UGET0110
C	ARGUMENTS	IOPT - OPTION PARAMETER. (INPUT)	UGET0120
C		IF IOPT=1, THE CURRENT INPUT AND OUTPUT UNIT IDENTIFIER VALUES ARE RETURNED IN NIN AND NOUT, RESPECTIVELY.	UGET0130
C		IF IOPT=2, THE INTERNAL VALUE OF NIN IS RESET FOR SUBSEQUENT USE.	UGET0140
C		IF IOPT=3, THE INTERNAL VALUE OF NOUT IS RESET FOR SUBSEQUENT USE.	UGET0150
C		NIN - INPUT UNIT IDENTIFIER.	UGET0160
C		OUTPUT IF IOPT=1, INPUT IF IOPT=2.	UGET0170
C		NOUT - OUTPUT UNIT IDENTIFIER.	UGET0180
C		OUTPUT IF IOPT=1, INPUT IF IOPT=3.	UGET0190
C			UGET0200
C			UGET0210
C			UGET0220
C			UGET0230
C			UGET0240
C			UGET0250
C			UGET0260
C			UGET0270
C	PRECISION/HARDWARE	- SINGLE/ALL	UGET0280
C			UGET0290
C	REQD. IMSL ROUTINES	- NONE REQUIRED	UGET0300
C			UGET0310
C	NOTATION	- INFORMATION ON SPECIAL NOTATION AND CONVENTIONS IS AVAILABLE IN THE MANUAL INTRODUCTION OR THROUGH IMSL ROUTINE UHELP	UGET0320
C			UGET0330
C			UGET0340
C			UGET0350
C	REMARKS	EACH IMSL ROUTINE THAT PERFORMS INPUT AND/OR OUTPUT OPERATIONS CALLS UGETIO TO OBTAIN THE CURRENT U IDENTIFIER VALUES. IF UGETIO IS CALLED WITH IOPT=1 OR IOPT=3, NEW UNIT IDENTIFIER VALUES ARE ESTABLISHED. SUBSEQUENT INPUT/OUTPUT IS PERFORMED ON THE NEW UNITS.	UGET0360
C			UGET0370
C			UGET0380
C			UGET0390
C			UGET0400
C			UGET0410
C	COPYRIGHT	- 1978 BY IMSL, INC. ALL RIGHTS RESERVED.	UGET0420
C			UGET0430
C	WARRANTY	- IMSL WARRANTS ONLY THAT IMSL TESTING HAS BEEN APPLIED TO THIS CODE. NO OTHER WARRANTY, EXPRESSED OR IMPLIED, IS APPLICABLE.	UGET0440
C			UGET0450
C			UGET0460
C			UGET0470
C	-----	-----	UGET0480
C	SUBROUTINE UGETIO (IOPT, NIN, NOUT)		UGET0490
C		SPECIFICATIONS FOR ARGUMENTS	UGET0500
C	INTEGER	IOPT, NIN, NOUT	UGET0510
C		SPECIFICATIONS FOR LOCAL VARIABLES	UGET0520
C	INTEGER	NIND, NOUTD	UGET0530
C	DATA	NIND/5/, NOUTD/6/	UGET0540
C		FIRST EXECUTABLE STATEMENT	UGET0550
	IF (IOPT.EQ.3) GO TO 10		UGET0560
	IF (IOPT.EQ.2) GO TO 5		UGET0570
	IF (IOPT.NE.1) GO TO 9005		UGET0580
	NIN = NIND		UGET0590
	NOUT = NOUTD		UGET0600
	GO TO 9005		UGET0610
			UGET0620

5 NIND = NIN
GO TO 9005
10 NOUTD = NOUT
9005 RETURN
END

UGET0630
UGET0640
UGET0650
UGET0660
UGET0670

C	IMSL ROUTINE NAME	- USPDK	USPK0010
C			USPK0020
C	-----		USPK0030
C			USPK0040
C	COMPUTER	- IBM/SINGLE	USPK0050
C			USPK0060
C	LATEST REVISION	- NOVEMBER 1, 1984	USPK0070
C			USPK0080
C	PURPOSE	- NUCLEUS CALLED BY IMSL ROUTINES THAT HAVE	USPK0090
C		CHARACTER STRING ARGUMENTS	USPK0100
C			USPK0110
C	USAGE	- CALL USPDK (PACKED, NCHARS, UNPAKD, NCHMTB)	USPK0120
C			USPK0130
C	ARGUMENTS	PACKED - CHARACTER STRING TO BE UNPACKED. (INPUT)	USPK0140
C		NCHARS - LENGTH OF PACKED. (INPUT) SEE REMARKS.	USPK0150
C		UNPAKD - INTEGER ARRAY TO RECEIVE THE UNPACKED	USPK0160
C		REPRESENTATION OF THE STRING. (OUTPUT)	USPK0170
C		. NCHMTB - NCHARS MINUS TRAILING BLANKS. (OUTPUT)	USPK0180
C			USPK0190
C	PRECISION/HARDWARE	- SINGLE/ALL	USPK0200
C			USPK0210
C	REQD. IMSL ROUTINES	- NONE	USPK0220
C			USPK0230
C	REMARKS	1. USPDK UNPACKS A CHARACTER STRING INTO AN INTEGER ARRAY	USPK0240
C		IN (A1) FORMAT.	USPK0250
C		2. UP TO 129 CHARACTERS MAY BE USED. ANY IN EXCESS OF	USPK0260
C		THAT ARE IGNORED.	USPK0270
C			USPK0280
C	COPYRIGHT	- 1984 BY IMSL, INC. ALL RIGHTS RESERVED.	USPK0290
C			USPK0300
C	WARRANTY	- IMSL WARRANTIES ONLY THAT IMSL TESTING HAS BEEN	USPK0310
C		APPLIED TO THIS CODE. NO OTHER WARRANTY,	USPK0320
C		EXPRESSED OR IMPLIED, IS APPLICABLE.	USPK0330
C			USPK0340
C	-----		USPK0350
C	SUBROUTINE USPDK	(PACKED, NCHARS, UNPAKD, NCHMTB)	USPK0360
C		SPECIFICATIONS FOR ARGUMENTS	USPK0370
C	INTEGER	NC, NCHARS, NCHMTB	USPK0380
C			USPK0390
C	LOGICAL*1	UNPAKD (1), PACKED (1), LBYTE, LBLANK	USPK0400
C	INTEGER*2	IBYTE, IBLANK	USPK0410
C	EQUIVALENCE	(LBYTE, IBYTE)	USPK0420
C	DATA	LBLANK /1H /	USPK0430
C	DATA	IBYTE /1H /	USPK0440
C	DATA	IBLANK /1H /	USPK0450
C		INITIALIZE NCHMTB	USPK0460
C	NCHMTB = 0		USPK0470
C		RETURN IF NCHARS IS LE ZERO	USPK0480
C	IF (NCHARS.LE.0) RETURN		USPK0490
C		SET NC=NUMBER OF CHARS TO BE DECODED	USPK0500
C	NC = MIN0 (129, NCHARS)		USPK0510
C	NWORDS = NC*4		USPK0520
C	J = 1		USPK0530
C	DO 110 I = 1, NWORDS, 4		USPK0540
C	UNPAKD (I) = PACKED (J)		USPK0550
C	UNPAKD (I+1) = LBLANK		USPK0560
C	UNPAKD (I+2) = LBLANK		USPK0570
C	UNPAKD (I+3) = LBLANK		USPK0580
C	110 J = J+1		USPK0590
C		CHECK UNPAKD ARRAY AND SET NCHMTB	USPK0600
C		BASED ON TRAILING BLANKS FOUND	USPK0610
C			USPK0620
C	DO 200 N = 1, NWORDS, 4		


```
      NN = NWORDS - N - 2
      LBYTE = UNPAKD(NN)
      IF (LBYTE .NE. IBLANK) GO TO 210
200  CONTINUE
      NN = 0
210  NCHMTB = (NN + 3) / 4
      RETURN
      END
```

```
USPK0630
USPK0640
USPK0650
USPK0660
USPK0670
USPK0680
USPK0690
USPK0700
```

LIST OF REFERENCES

1. von Braun, W. and Ordway, F., *History of Rocketry and Space Travel*, 3d ed., T. Crowell Co., 1974.
2. Sutton, G.P., *Rocket Propulsion Elements*, 4th ed., John Wiley & Sons, 1976.
3. Jahn, R.G., *Physics of Electric Propulsion*, McGraw-Hill, 1968.
4. Sutton, G.P., *Rocket Propulsion Elements*, 5th ed., John Wiley & Sons, 1986.
5. Stuhlinger, E., *Ion Propulsion for Space Flight*, McGraw-Hill, 1964.
6. Myers, R.M., Manteniaks, M.A., and LaPointe, M.R., *MPD Thruster Technology*, NASA-TM-105242, AIAA-91-3568, Sept., 1968.
7. Myers, R.M., *Applied-Field MPD Thruster Geometry Effects*, AIAA-91-2342, June, 1991.
8. Saber, A.J., "Anode Power in the Quasi-Steady MPD (Magnetoplasmadynamic) Thruster," Ph.D. Thesis, Princeton Univ., NJ, 1974.
9. Shih, K.T., Pfender, E., Ibele, W.E., and Eckert, E.R.G., "Experimental Anode Heat-Transfer Studies in a Coaxial Arc Configuration," *AIAA Journal*, V. 6, No. 8, pp.1482-1487, August, 1968.
10. Sanders, N.A., and Pfender, E., "Measurement of the Anode Falls and Anode Heat Transfer in Atmospheric Pressure, High Intensity Arcs," *J. Appl. Phys.*, V. 55, No. 3, pp. 714-722, Feb., 1984.
11. Vainberg, L.I., Lyubimov, G.A., and Smolin, G.G., "High Current Discharge Effects and Anode Damage in an End-Fire Plasma Accelerator," *Sov. Physics, Tech. Phys.*, V. 23, No. 4, pp. 439-443, April, 1978.
12. Hugel, H., "Effects of Self-Magnetic Forces on the Anode Mechanism of a High Current Discharge," *IEEE Trans. Plasma Sci.*, V. PS-8, No. 4, pp.437-442, Dec. 1980.
13. Gallimore, A.D., Kelly, A.J., and Jahn, R.G., "Anode Power Deposition in Quasisteady MPD Thrusters," *J. Propulsion & Pwr.*, V. 8, No. 6, pp. 1224-1231, Dec., 1992.

14. Dolson, R.C., and Biblarz, O., "Analysis of the Voltage Drop Arising from a Collision-dominated Sheath," *J. Appl. Phys.*, V. 47, No. 12, pp. 5280-5287, Dec., 1976.
15. Myers, R.M., "Energy Deposition in Low Power Coaxial Plasma Thrusters," Ph.D. Thesis, Princeton Univ., NJ, June, 1989.
16. Oberth, R.C., and Jahn, R.G., "Anode Phenomena in High-Current Accelerators," *AIAA Journal*, V. 10, No. 1, pp. 86-91, Jan., 1972.
17. Slezione, P.C., Auweter-Kurtz, M., and Schrade, H.O., "Numerical Codes for Cylindrical MPD Thrusters," IEPC 88-038, 20th Int'l. Elec. Prop. Conf., Garmisch-Partenkirchen, W. Germany, Oct., 1988.
18. Slezione, P.C., Auweter-Kurtz, M., and Schrade, H.O., "Numerical Evaluation of MPD Thrusters," *AIAA 90-2602*, July, 1990.
19. LaPointe, M.R., "Numerical Simulation of Self-Field MPD Thrusters," *AIAA-91-2341*, NASA-CR-187168, July, 1991.
20. Subramaniam, V.V., and Lawless, J.L., "Thermal Instabilities of the Anode in a Magnetoplasmadynamic Thruster," *J. Propulsion & Pwr.*, V. 6, No. 2, pp. 221-224, Mar., 1990.
21. Biblarz, O., "Approximate Sheath Solutions for a Planar Plasma Anode," *IEEE Trans. Plasma Sci.*, V. 19, No. 6, pp. 1235-1243, Dec., 1991.
22. Biblarz, O., Dolson, R.G., and Shorb, R.C., "Anode Phenomena a Collision-dominated Plasma," *J. Appl. Phys.*, V. 46, No. 8, pp. 3342-3346, Aug., 1975.
23. Rudolph, L.K. and Pawlik, E.V., "The MPD Thruster Development Program," AIAA Technical Paper 79-2050, in *Progress in Aeronautics and Astronautics*, Vol. 79, Amer. Inst of Aer. & Astro., 1981.
24. Cann, G.L., and Marlotte, G.L., "Hall Current Plasma Accelerator," *AIAA Journal*, V. 2, No. 7, pp. 1234-1241, Jul., 1964.
25. Brophy, J., *Stationary Plasma Thruster Evaluation in Russia, Summary Report*, Jet Propulsion Laboratory (JPL) Publication 92-4, March 15, 1992.
26. Mitchner, M., and Kruger, C.H., *Partially Ionized Gases*, pp. 128-134, Wiley, 1973.
27. Cobine, J.D., *Gaseous Conductors, Theory and Engineering Applications*, McGraw-Hill, 1941.

28. von Engel, A., *Ionized Gases*, Clarendon Press, 1965.
29. Chen, F.F., *Introduction to Plasma Physics and Controlled Fusion*, 2nd ed., p.10, Plenum, 1984.
30. Lin, S., Resler, E., and Kantrowitz, A., "Electrical Conductivity of Highly Ionized Argon Produced by Shock Waves," *J. Appl. Phys.*, V. 26, p. 95, Jan., 1955.
31. Campbell, A., *Plasma Physics and Magnetofluidmechanics*, p. 161, McGraw-Hill, 1963.
32. Nasser, E., *Fundamentals of Gaseous Ionization and Plasma Electronics*, p.412, Wiley, 1971.
33. Ecker, G., "Anode Spot Instability. I. The Homogeneous Short Gap Instability," *IEEE Trans. Plasma Sci.*, V. PS-2, No. 3, Sept., 1974.
34. Biblarz, O. and Riggs, J.F., "Anode Sheath Contributions in Plasma Thrusters," *AIAA 93-2495*, Jun., 1993.
35. Miller, H.C., "Vacuum Arc Anode Phenomena," *IEEE Trans. Plasma Sci.*, V. PS-11, No. 2, June, 1983.
36. Miller, H.C., "Discharge Modes at the Anode of a Vacuum Arc," *IEEE Trans. Plasma Sci.*, V. PS-11, No. 3, pp. 122-127, Sep., 1983.
37. Rich, J.A., Prescott, L.E., and Cobine, J.D., "Anode Phenomena in Metal-Vapor Arcs at High Currents," *J. Appl. Phys.*, V. 12, No. 12, pp.587-601, Feb., 1971.
38. Schuocker, D., "Improved Model for Anode Spot Formation in Vacuum Arcs," *IEEE Trans. Plasma Sci.*, V. PS-7, No. 4, pp. 209-216, Dec., 1979.
39. Gear, C.W., *Numerical Initial Value Problems in Ordinary Differential Equations*, Prentice-Hall, Englewood Cliffs, NJ, 1971.
40. Burnet, H., Vincent, P., and Rocca Serra, J., "Ionization Mechanism in a Nitrogen Glow Discharge," *J. Appl. Phys.*, V. 54, No. 9, pp. 4951-4957, 1983.
41. Phelps, A.P. and Pitchford, L.C., "Anisotropic Scattering Electrons by N₂ and its Effect on Electron Transport," *Phys. Rev. A*, V. 31, pp. 2932-2949, 1985.
42. Myers, R.M., Kelly, A.J. and Jahn, R.G., "Energy Deposition in Low-Power Coaxial Thrusters," *J. Propulsion*, V. 7, No. 5, pp. 732-739, Sep./Oct., 1991.

43. Biblarz, O., "Thermionic Arc Initiation", *1992 IEEE International Conference on Plasma Science, Tampa, FL*, June 1992.
44. Gallimore, A.D., "Anode Power Deposition in Coaxial MPD Thrusters," Ph.D. Thesis, Princeton Univ., NJ, Oct., 1992.
45. Biblarz, O. and Barto, J.L., "Fluid-Dynamic Effects, Including Turbulence, on a High Pressure Discharge". *Gas Flow and Chemical Lasers*, 6th Int. Symposium (S. Rosenwaks, Ed.), pp. 34-39, Springer-Verlag, Berlin, 1987.
46. Park, W. & Choi, D., "Numerical Analysis of MPD Arcs for Plasma Acceleration," *IEEE Trans. Plasma Sci.*, V. PS-15, No. 5, pp. 618-624, Oct., 1987.
47. Schoeck, P. A., Eckert, E.R.G., and Wutzke, S.A., "An Investigation of the Anode Losses in Argon Arcs and their Reduction by Transpiration Cooling," *ARL 62-341, DTIC AD-278570*, April, 1962.
48. Brady, J.E., *General Chemistry, Principles & Structure*, 5th ed., Wiley, 1990, p. 223.
49. Janes, G.S., "Magnetohydrodynamic Propulsion," in *Advanced Propulsion Techniques*, AGARD Proceedings, Aug., 1960, pp. 151-154, Pergamon, 1961.
50. Connolly, D.J., Sovie, R.J., Michels, C.J., and Burkhart, J.A., "Low Environmental Pressure MPD Arc Tests," *AIAA Journal*, V. 6, No. 7, pp. 1271-1276, July, 1968.
51. Subramaniam, V.V., "Fundamental Studies on Erosion in MPD Thrusters," *AFOSR 87-0360*, April, 1992.
52. Hurwics, H. and Rogan, J. E., "High Temperature Thermal Protection Systems", Section 19, , *Handbook of Heat Transfer* (Rohsenow, W.M., and Hartnett, J.P., Eds) McGraw-Hill, 1973.
53. Kuriki, K. and Suzuki, H., "Quasisteady MPD Arcjet with Anode Gas Injection," *AIAA 79-2058, 14th International Electric Propulsion Conference, Princeton, NJ*, Oct., 1979.
54. Sutton, G.W. and Sherman A., *Engineering Magnetohydrodynamics*, p. 148, McGraw-Hill, 1965.
55. Choueiri, E.Y., Kelly, A.J., and Jahn, R.G., "Mass Savings Domain of Plasma Propulsion for LEO to GEO Transfer," *J. Spacecraft and Rockets*, V. 30, No. 6, pp. 749-754, Nov./Dec., 1993.

INITIAL DISTRIBUTION LIST

1. **Defense Technical Information Center** 2
Cameron Station
Alexandria, Virginia 22304-6145
2. **Library, Code 52** 2
Naval Postgraduate School
Monterey, California 93943-5002
3. **Chairman** 1
Department of Aeronautics & Astronautics, Code AA
Naval Postgraduate School
Monterey, California 93943-5000
4. **Professor Oscar Biblarz** 3
Department of Aeronautics & Astronautics, Code AA/Bi
Naval Postgraduate School
Monterey, California 93943-5000
5. **Professor Fred Schwirzke** 1
Department of Physics, Code PH/Sw
Naval Postgraduate School
Monterey, California 93943-5000
6. **Commander, Space & Naval Warfare Systems Command** 1
Space Technology Directorate (SPAWAR-40)
2451 Crystal Drive
Arlington, Virginia 22245-5200
7. **Dr. Roger Myers** 1
Lewis Research Center
M.S. SPTD-1
Cleveland, Ohio 44135-3191
8. **Dr. James S. Sovey** 1
SPTD
NASA Lewis Research Center
21000 Brookpark Rd.
Cleveland, Ohio 44135

9. Dr. Tom Pivrotto 1
Jet Propulsion Laboratory
4800 Oak Grove Dr.
Pasadena, California 91109
M.S.125-224
10. Dr. John Brophy 1
Jet Propulsion Laboratory
4800 Oak Grove Dr.
Pasadena, California 91109
M.S.125-224
11. Dr. Jay Polk 1
Jet Propulsion Laboratory
4800 Oak Grove Dr.
Pasadena, California 91109
M.S.125-224
12. Dr. Arnold J. Kelly 1
Dept. of Mechanical & Aerospace Engineering
Princeton University
Princeton, New Jersey 08544
13. Dr. Mitat A. Birkan 1
AFOSR NA
110 Duncan Avenue, Suite B115
Bolling AFB, D.C. 20352-0001
14. Dr. Ed Weiler 1
Code SZB
NASA Headquarters
Washington, D.C. 20546-0001
15. LCDR John Riggs 5
10215 Centinella Dr.
La Mesa, California 91941